SIAM J. SCI. COMPUT.
Vol. 42, No. 3, pp. A1860–A1884

A POSTERIORI ERROR ESTIMATES FOR THE STATIONARY NAVIER–STOKES EQUATIONS WITH DIRAC MEASURES*

ALEJANDRO ALLENDES†, ENRIQUE OTÁROLA†, AND ABNER J. SALGADO‡

Abstract. In two dimensions, we propose and analyze an a posteriori error estimator for finite element approximations of the stationary Navier–Stokes equations with singular sources on Lipschitz, but not necessarily convex, polygonal domains. Under a smallness assumption on the continuous and discrete solutions, we prove that the devised error estimator is reliable and locally efficient. We illustrate the theory with numerical examples.

Key words. a posteriori error estimates, Navier–Stokes equations, Dirac measures, Muckenhoupt weights

AMS subject classifications. 35Q35, 35Q30, 35R06, 76D05, 65N15, 65N30, 65N50

DOI. 10.1137/19M1292436

1. Introduction.

Let $\Omega \subset \mathbb{R}^2$ be an open and bounded domain with Lipschitz boundary $\partial\Omega$. In this work we will be interested in the design and analysis of a posteriori error estimates for finite element approximations of the stationary Navier–Stokes problem

$$-\Delta \mathbf{u} + (\mathbf{u}\cdot\nabla)\mathbf{u} + \nabla \mathsf{p} = \mathbf{F}\delta_z \text{ in } \Omega, \qquad \operatorname{div}\mathbf{u} = 0 \text{ in } \Omega, \qquad \mathbf{u} = \mathbf{0} \text{ on } \partial\Omega, \tag{1}$$

where δ_z corresponds to the Dirac delta supported at the interior point $z \in \Omega$ and $\mathbf{F} \in \mathbb{R}^2$. Here, $\mathbf{u}$ represents the velocity of the fluid, p represents the pressure, and $\mathbf{F}\delta_z$ is an externally applied force. Notice that, for the sake of simplicity, we have taken the viscosity to be equal to one.

Since the stationary Navier–Stokes equations model the motion of a stationary, incompressible, Newtonian fluid, it is no surprise that their analysis and approximation, at least in energy-type spaces, is very well developed; see, for instance, [41, 24, 10, 39, 40] for an account of this theory.

On the other hand, there are situations where one wishes to allow this model to be driven by singular forces, like in (1). As a first example of this, in the linear setting, one must mention that in the case that $\mathbf{F}$ belongs to the canonical basis of $\mathbb{R}^2$, then we obtain entries of the Green's matrix for the Stokes problem. Every situation where the Green's matrix needs to be computed or approximated requires the solution of the linear version of (1). Keeping the problem linear, [31] argues that these equations can be used to model the movement of active thin structures in a viscous fluid. A

*Submitted to the journal's Methods and Algorithms for Scientific Computing section October 10, 2019; accepted for publication (in revised form) March 30, 2020; published electronically June 29, 2020.

https://doi.org/10.1137/19M1292436

Funding: The work of the first author was partially supported by CONICYT through FONDECYT project 1170579. The work of the second author was partially supported by CONICYT through FONDECYT project 11180193. The work of the third author was partially supported by NSF grant DMS-1720213.

†Departamento de Matemática, Universidad Técnica Federico Santa María, 2390123 Valparaíso, Chile (alejandro.allendes@usm.cl, http://aallendes.mat.utfsm.cl/, enrique.otarola@usm.cl, http://eotarola.mat.utfsm.cl/).

‡Department of Mathematics, University of Tennessee, Knoxville, TN 37996 (asalgad1@utk.edu, http://www.math.utk.edu/~abnersg).

numerical scheme is proposed, but no complete analysis of this method is provided. Local error estimates, away from the support of the delta, were later derived in [9].

A second example comes from PDE-constrained optimization (optimal control). Reference [12] sets up a problem where the state is governed by the stationary Navier–Stokes equations, but with a forcing (control) that is measure valued, like in (1). The motivation behind this is what the authors denote *sparsity* of the control, meaning that its support is small, even allowing it to have Lebesgue measure zero. The analysis of [12] assumes that the domain has C^2 boundary and seeks a solution to (1) in $\mathbf{W}_0^{1,q}(\Omega) \times L^q(\Omega)/\mathbb{R}$ with $q \in [4/3, 2)$. In this setting a complete existence theory for the state is provided, and the optimization problem is analyzed. Necessary and sufficient optimality conditions are deduced. Reference [12], however, is not concerned with approximation.

In this work we continue our program aimed at developing numerical methods for models of fluids under singular forces. The guiding principle that we follow is that by introducing a weight, and working in the ensuing weighted function spaces, we can allow for data that is singular, so that (1) fits our theory. We immediately must comment that the literature already presents an analysis of the stationary Navier–Stokes equations on Muckenhoupt weighted spaces; see [37]. That paper, however, requires the domain to be $C^{1,1}$, which is not suitable for a finite element approximation. We, in contrast, assume only that the domain is Lipschitz. In [34] we developed existence and uniqueness for the Stokes problem over a reduced class of weighted spaces; see Definition 1 below. The numerical analysis of this linear model is presented in [19, 5], where a priori and a posteriori, respectively, error analyses are discussed. The nonlinear case, that is, (1), is considered in [35], where existence and uniqueness for small data, and in the same functional setting, is proved. In the setting of uniqueness, an a priori error analysis for a numerical scheme is also developed. This brings us to the current work and its contributions. The solution to (1), because of the singular data, is not expected to be smooth, and thus adaptive methods must be developed to efficiently approximate it. Our goal here is to develop and analyze a reliable and efficient a posteriori error estimator, and show its performance when used in a standard adaptive procedure.

Before proceeding any further, we must make a comment about our choice of boundary conditions, as practical problems usually prescribe nonhomogeneous or other types of boundary conditions. While nonhomogeneous Dirichlet conditions could be considered, traces of weighted spaces are not easily characterized; see [43, 44] and [11, section 2.2.1]. Thus, it is not easy to describe what type of Dirichlet data is admissible. On the other hand, the existence theory for the stationary Navier–Stokes equations on weighted spaces with other types of boundary conditions has not been developed. One of the main issues is again that traces of weighted spaces cannot be easily characterized. This would limit the type of data $\mathbf{g}$ that can be used in, say, natural boundary conditions of the form

$$(\nabla \mathbf{u} - p\mathbf{I}) \cdot \mathbf{n} = \mathbf{g}$$

on a piece of the boundary. In addition, the inf-sup condition for the pressure is not known on weighted spaces if the velocity space consists of functions that vanish only on a piece of the boundary.

Our presentation will be organized as follows. We set notation in section 2, where we also recall the definition of Muckenhoupt weights and introduce the weighted spaces we shall work with. In section 3, we introduce a suitable weak formulation for problem (1) in weighted spaces and review existence and uniqueness results for small

data. Section 4 presents basic ingredients of finite element methods. Section 5 is one of the highlights of our work. In section 5.1 we introduce a Ritz projection of the residuals, and in section 5.2 we prove that the energy norm of the error can be bounded in terms of the energy norm of the Ritz projection. We thus propose in section 5.3 an a posteriori error estimator for inf-sup stable finite element approximations of problem (1); the devised error estimator is proven to be locally efficient and globally reliable. Section 6 presents a series of numerical experiments that illustrate and extend our theory. We conclude in section 7 by providing a summary of our developments, our numerical findings, and what we think might be the limitations of our approach.

2. Notation and preliminaries. Let us set notation and describe the setting we shall operate with. Throughout this work $\Omega \subset \mathbb{R}^2$ is an open and bounded polygonal domain with Lipschitz boundary $\partial\Omega$. Notice that we do not assume that Ω is convex. If $\mathcal{W}$ and $\mathcal{Z}$ are Banach function spaces, we write $\mathcal{W} \hookrightarrow \mathcal{Z}$ to denote that $\mathcal{W}$ is continuously embedded in $\mathcal{Z}$. We denote by $\mathcal{W}'$ and $\|\cdot\|_{\mathcal{W}}$ the dual and the norm of $\mathcal{W}$, respectively.

For $E \subset \bar{\Omega}$ of finite Hausdorff i-dimension, $i \in \{1, 2\}$, we denote its measure by $|E|$. If E is such a set and $f : E \to \mathbb{R}$, we denote the mean value of f by

$$\fint_E f = \frac{1}{|E|} \int_E f.$$

The relation $a \lesssim b$ indicates that $a \leq Cb$, with a constant C that depends neither on a, b nor on the discretization parameters. The value of C might change at each occurrence.

2.1. Weights. A notion which will be fundamental for further discussions is that of a weight. By a weight we mean a locally integrable, nonnegative function defined on $\mathbb{R}^2$. Of particular interest in our constructions will be weights that belong to the Muckenhoupt class A_2 [17], which consist of all weights ω such that

$$[\omega]_{A_2} := \sup_B \left(\fint_B \omega \right) \left(\fint_B \omega^{-1} \right) < \infty, \tag{2}$$

where the supremum is taken over all balls B in $\mathbb{R}^2$. For $\omega \in A_2$ the quantity $[\omega]_{A_2}$ is the Muckenhoupt characteristic of ω. We refer the reader to [17, 25, 33, 42] for basic facts about the class A_2. An A_2 weight which will be essential for our subsequent developments is the following. Let $z \in \Omega$ and $\alpha \in (-2, 2)$. Then

$$\mathsf{d}_z^\alpha(x) = |x - z|^\alpha \in A_2. \tag{3}$$

An important property of the weight d_z^α is that there is a neighborhood of $\partial\Omega$ where d_z^α is strictly positive and continuous. This observation motivates us to define a restricted class of Muckenhoupt weights [23, Definition 2.5].

DEFINITION 1 (class $A_2(\Omega)$). *Let $\Omega \subset \mathbb{R}^2$ be a Lipschitz domain. We say that $\omega \in A_2$ belongs to $A_2(\Omega)$ if there are an open set $\mathcal{G} \subset \Omega$ and $\varepsilon, \omega_l > 0$ such that*

$$\{x \in \Omega : \operatorname{dist}(x, \partial\Omega) < \varepsilon\} \subset \mathcal{G}, \qquad \omega_{|\bar{\mathcal{G}}} \in C(\bar{\mathcal{G}}), \qquad \omega_l \leq \omega(x) \quad \forall x \in \bar{\mathcal{G}}.$$

As we have mentioned in the introduction, what allows us to consider rough forcings in (1) is the use of weights and weighted spaces, as we will define below. We must note, however, that since we are not assuming our polygonal domain Ω

to be convex, the same considerations given in the counterexample of [16, page 2] show that we cannot work with general weights, and we cannot allow our forcings to have singularities near the boundary. This is the importance of the class $A_2(\Omega)$ of Definition 1.

2.2. Weighted spaces. Let E be an arbitrary domain in $\mathbb{R}^2$ and $\omega \in A_2$. We define $L^2(\omega, E)$ as the space of Lebesgue measurable functions in E such that

$$\|v\|_{L^2(\omega,E)} = \left(\int_E \omega |v|^2\right)^{\frac{1}{2}} < \infty.$$

We define the weighted Sobolev space $H^1(\omega, E)$ as the set of functions $v \in L^2(\omega, E)$ such that, for every multi-index $\gamma \in \mathbb{N}_0^2$ with $|\gamma| \leq 1$, we have that the distributional derivatives $D^\gamma v \in L^2(\omega, E)$. We endow $H^1(\omega, E)$ with the norm

$$\|v\|_{H^1(\omega,E)} := \left(\|v\|^2_{L^2(\omega,E)} + \|\nabla v\|^2_{L^2(\omega,E)}\right)^{\frac{1}{2}}. \tag{4}$$

We define $H_0^1(\omega, E)$ as the closure of $C_0^\infty(E)$ in $H^1(\omega, E)$. We notice that, owing to a weighted Poincaré inequality [22, 13, 28], over $H_0^1(\omega, E)$ the seminorm $\|\nabla v\|_{L^2(\omega,E)}$ is equivalent to the norm defined in (4).

Spaces of vector valued functions will be denoted by boldface, that is,

$$\mathbf{H}_0^1(\omega, E) = [H_0^1(\omega, E)]^2, \quad \|\nabla \mathbf{v}\|_{\mathbf{L}^2(\omega,E)} := \left(\sum_{i=1}^2 \|\nabla v_i\|^2_{L^2(\omega,E)}\right)^{\frac{1}{2}},$$

where $\mathbf{v} = (v_1, v_2)^\intercal$.

The following product spaces with the weight d_z^α will be of particular importance. For $\alpha \in (-2, 2)$, we define

$$\mathcal{X}(E) = \mathbf{H}_0^1(\mathsf{d}_z^\alpha, E) \times L^2(\mathsf{d}_z^\alpha, E)/\mathbb{R}, \quad \mathcal{Y}(E) = \mathbf{H}_0^1(\mathsf{d}_z^{-\alpha}, E) \times L^2(\mathsf{d}_z^{-\alpha}, E)/\mathbb{R}, \tag{5}$$

which we endow with standard product space norms. When $E = \Omega$, and in order to simplify the presentation of the material, we write $\mathcal{X} = \mathcal{X}(\Omega)$ and $\mathcal{Y} = \mathcal{Y}(\Omega)$.

3. The stationary Navier–Stokes equations under singular forcing. For $\alpha \in (-2, 2)$, we define the bilinear forms

$$a : \mathbf{H}_0^1(\mathsf{d}_z^\alpha, \Omega) \times \mathbf{H}_0^1(\mathsf{d}_z^{-\alpha}, \Omega) \to \mathbb{R}, \quad a(\mathbf{w}, \mathbf{v}) := \int_\Omega \nabla \mathbf{w} : \nabla \mathbf{v}, \tag{6}$$

and

$$b_\pm : \mathbf{H}_0^1(\mathsf{d}_z^{\pm\alpha}, \Omega) \times L^2(\mathsf{d}_z^{\mp\alpha}, \Omega) \to \mathbb{R}, \quad b_\pm(\mathbf{v}, q) := -\int_\Omega q \operatorname{div} \mathbf{v}. \tag{7}$$

We also define the trilinear form

$$c : [\mathbf{H}_0^1(\mathsf{d}_z^\alpha, \Omega)]^2 \times \mathbf{H}_0^1(\mathsf{d}_z^{-\alpha}, \Omega) \to \mathbb{R}, \quad c(\mathbf{u}, \mathbf{w}; \mathbf{v}) := -\int_\Omega \mathbf{u} \otimes \mathbf{w} : \nabla \mathbf{v}. \tag{8}$$

The results of [34] yield an inf-sup condition for the bilinear form a on weighted spaces; i.e., we have

$$\begin{aligned} \inf_{0\neq \mathbf{v}\in \mathbf{H}_0^1(\mathsf{d}_z^\alpha,\Omega)} \sup_{0\neq \mathbf{w}\in \mathbf{H}_0^1(\mathsf{d}_z^{-\alpha},\Omega)} \frac{a(\mathbf{v},\mathbf{w})}{\|\nabla \mathbf{v}\|_{\mathbf{L}^2(\mathsf{d}_z^\alpha,\Omega)} \|\nabla \mathbf{w}\|_{\mathbf{L}^2(\mathsf{d}_z^{-\alpha},\Omega)}} \\ = \inf_{0\neq \mathbf{w}\in \mathbf{H}_0^1(\mathsf{d}_z^{-\alpha},\Omega)} \sup_{0\neq \mathbf{v}\in \mathbf{H}_0^1(\mathsf{d}_z^\alpha,\Omega)} \frac{a(\mathbf{v},\mathbf{w})}{\|\nabla \mathbf{v}\|_{\mathbf{L}^2(\mathsf{d}_z^\alpha,\Omega)} \|\nabla \mathbf{w}\|_{\mathbf{L}^2(\mathsf{d}_z^{-\alpha},\Omega)}} > 0. \end{aligned} \tag{9}$$

On the other hand, since we are in two dimensions and $\mathsf{d}_z^\alpha \in A_2$, [22, Theorem 1.3] shows that $\mathbf{H}^1_0(\mathsf{d}_z^\alpha,\Omega) \hookrightarrow \mathbf{L}^4(\mathsf{d}_z^\alpha,\Omega)$. Thus, if we denote by $C_{4\to 2}$ the best embedding constant, we have that the convective term can be bound as follows:

$$
\begin{aligned}
|c(\mathbf{u},\mathbf{w};\mathbf{v})| = \left|\int_\Omega \mathbf{u}\otimes\mathbf{w} : \nabla\mathbf{v}\right| &\leq \|\mathbf{u}\|_{\mathbf{L}^4(\mathsf{d}_z^\alpha,\Omega)}\|\mathbf{w}\|_{\mathbf{L}^4(\mathsf{d}_z^\alpha,\Omega)}\|\nabla\mathbf{v}\|_{\mathbf{L}^2(\mathsf{d}_z^{-\alpha},\Omega)} \\
&\leq C_{4\to 2}^2\|\nabla\mathbf{u}\|_{\mathbf{L}^2(\mathsf{d}_z^\alpha,\Omega)}\|\nabla\mathbf{w}\|_{\mathbf{L}^2(\mathsf{d}_z^\alpha,\Omega)}\|\nabla\mathbf{v}\|_{\mathbf{L}^2(\mathsf{d}_z^{-\alpha},\Omega)}.
\end{aligned} \tag{10}
$$

Remark 2 (two dimensions). Estimate (10) is the sole reason why our analysis is restricted to two dimensions. In three dimensions, since $\mathsf{d}_z^\alpha \in A_2$, we only have that $\mathbf{H}^1_0(\mathsf{d}_z^\alpha,\Omega) \hookrightarrow \mathbf{L}^{3+\delta}(\mathsf{d}_z^\alpha,\Omega)$, where $\delta > 0$; see [22, Theorem 1.3]. This is not enough to guarantee the boundedness of the convective term.

3.1. Weak formulation. With definitions (6)–(8) at hand, we consider the following weak formulation for problem (1): Find $(\mathbf{u},\mathsf{p}) \in \mathcal{X}$ such that

$$
a(\mathbf{u},\mathbf{v}) + b_-(\mathbf{v},\mathsf{p}) + c(\mathbf{u},\mathbf{u};\mathbf{v}) = \langle \mathbf{F}\delta_z,\mathbf{v}\rangle, \qquad b_+(\mathbf{u},q) = 0, \tag{11}
$$

for all $(\mathbf{v},q) \in \mathcal{Y}$. Here and in what follows $\langle\cdot,\cdot\rangle$ denotes a duality pairing. The spaces used for such pairing shall be evident from the context. We must immediately comment that in order to guarantee that $\delta_z \in H^1_0(\mathsf{d}_z^{-\alpha},\Omega)'$, and thus that $\langle \mathbf{F}\delta_z,\mathbf{v}\rangle$ is well-defined for $\mathbf{v} \in \mathbf{H}^1_0(\mathsf{d}_z^{-\alpha},\Omega)$, the parameter α should be restricted to belong to the interval $(0,2)$; see [30, Lemma 7.1.3] and [26, Remark 21.18].

3.2. Existence and uniqueness for small data. Let us define the mappings $\mathcal{S} : \mathcal{X} \to \mathcal{Y}'$, $\mathcal{NL} : \mathcal{X} \to \mathcal{Y}'$, and $\mathcal{F} \in \mathcal{Y}'$ by

$$
\begin{aligned}
\langle \mathcal{S}(\mathbf{u},p),(\mathbf{v},q)\rangle &= a(\mathbf{u},\mathbf{v}) + b_-(\mathbf{v},p) + b_+(\mathbf{u},q), \\
\langle \mathcal{NL}(\mathbf{u},p),(\mathbf{v},q)\rangle &= c(\mathbf{u},\mathbf{u};\mathbf{v}),
\end{aligned}
$$

and $\langle \mathcal{F},(\mathbf{v},q)\rangle = \langle \mathbf{F}\delta_z,\mathbf{v}\rangle$, respectively. With this notation (11) can be equivalently written as the following operator equation in $\mathcal{Y}'$:

$$
\mathcal{S}(\mathbf{u},p) + \mathcal{NL}(\mathbf{u},p) = \mathcal{F}.
$$

In what follows, by $\|\mathcal{S}^{-1}\|$ we shall denote the $\mathcal{Y}' \to \mathcal{X}$ norm of $\mathcal{S}^{-1}$. We recall that $C_{4\to 2}$ denotes the best constant in the embedding $\mathbf{H}^1_0(\mathsf{d}_z^\alpha,\Omega) \hookrightarrow \mathbf{L}^4(\mathsf{d}_z^\alpha,\Omega)$. Throughout this work, and without explicitly mentioning it, we assume that the forcing term $\mathbf{F}\delta_z$ is sufficiently small so that

$$
C_{4\to 2}^2\|\mathcal{S}^{-1}\|^2\|\mathbf{F}\delta_z\|_{\mathbf{H}^1_0(\mathsf{d}_z^{-\alpha},\Omega)'} < \frac{1}{6}. \tag{12}
$$

With this assumption on the data at hand, we have existence and uniqueness.

PROPOSITION 3 (existence and uniqueness). *Let Ω be Lipschitz and $\alpha \in (0,2)$. Assume that the intensity of the forcing term $\mathbf{F}$ is sufficiently small so that* (12) *holds. Then, there is a unique solution of* (11)*. Moreover, this solution satisfies the estimates*

$$
\|\nabla\mathbf{u}\|_{\mathbf{L}^2(\mathsf{d}_z^\alpha,\Omega)} \leq \frac{3}{2}\|\mathcal{S}^{-1}\|\ \|\mathbf{F}\delta_z\|_{\mathbf{H}^1_0(\mathsf{d}_z^{-\alpha},\Omega)'} \tag{13}
$$

and

$$
\|\mathsf{p}\|_{L^2(\mathsf{d}_z^\alpha,\Omega)} \lesssim \|\nabla\mathbf{u}\|_{\mathbf{L}^2(\mathsf{d}_z^\alpha,\Omega)} + \|\nabla\mathbf{u}\|^2_{\mathbf{L}^2(\mathsf{d}_z^\alpha,\Omega)} + \|\mathbf{F}\delta_z\|_{\mathbf{H}^1_0(\mathsf{d}_z^{-\alpha},\Omega)'},
$$

where the hidden constant is independent of $\mathbf{u}$, p, and $\mathbf{F}\delta_z$, but depends on α and blows up as either $\alpha \downarrow 0$ or $\alpha \uparrow 2$.

Proof. Existence, uniqueness, and the velocity estimate are the content of [35, Corollary 1]. To show the estimate on the pressure, we invoke the weighted inf-sup condition [18, Theorem 3.1], [36, Theorem 1], [19, Lemma 6.1]

$$\|p\|_{L^2(\mathsf{d}_z^\alpha,\Omega)} \lesssim \sup_{\mathbf{0}\neq\mathbf{v}\in\mathbf{H}_0^1(\mathsf{d}_z^{-\alpha},\Omega)} \frac{b_-(\mathbf{v},p)}{\|\nabla\mathbf{v}\|_{\mathbf{L}^2(\mathsf{d}_z^{-\alpha},\Omega)}} \quad \forall p\in L^2(\mathsf{d}_z^\alpha,\Omega)/\mathbb{R}.$$

The hidden constant depends only on Ω and $[\mathsf{d}_z^\alpha]_{A_2}$. Using this estimate for p, the first equation in (11), and the estimate on the convective term of (10), we obtain the desired pressure estimate. ∎

4. Discretization. We now propose a finite element scheme to approximate the solution to (11). To accomplish this task, we first introduce some terminology and a few basic ingredients.

4.1. Triangulation. We denote by $\mathscr{T}=\{T\}$ a conforming partition of $\bar\Omega$ into closed triangles T with size $h_T=\operatorname{diam}(T)$ and define $h_{\mathscr{T}}=\max_{T\in\mathscr{T}} h_T$. We denote by $\mathbb{T}$ the collection of conforming and shape regular meshes that are refinements of an initial mesh $\mathscr{T}_0$ [14, 21].

We denote by $\mathscr{S}$ the set of internal one dimensional interelement boundaries S of $\mathscr{T}$. For $S\in\mathscr{S}$, we indicate by h_S the length of S. If $T\in\mathscr{T}$, we define $\mathscr{S}_T$ as the subset of $\mathscr{S}$ that contains the sides of T. For $S\in\mathscr{S}$, we set $\mathcal{N}_S=\{T^+,T^-\}$, where $T^+,T^-\in\mathscr{T}$ are such that $S=T^+\cap T^-$. For $T\in\mathscr{T}$, we define the following *stars* or *patches* associated with the element T:

$$\mathcal{N}_T := \{T'\in\mathscr{T} : \mathscr{S}_T\cap\mathscr{S}_{T'}\neq\emptyset\}, \qquad \mathcal{S}_T := \{T'\in\mathscr{T} : T\cap T'\neq\emptyset\}. \tag{14}$$

Thus, $\mathcal{N}_T$ contains the (at most) three triangles that share a side with T, while $\mathcal{S}_T$ is $\mathcal{N}_T$ together with those triangles that also share a vertex with T. In an abuse of notation, in what follows, by $\mathcal{N}_T$ and $\mathcal{S}_T$ we will indistinctively denote either these sets or the union of the triangles that comprise them.

4.2. Finite element spaces. Given a mesh $\mathscr{T}\in\mathbb{T}$, we denote by $\mathbf{V}(\mathscr{T})$ and $\mathcal{P}(\mathscr{T})$ the finite element spaces that approximate the velocity field and the pressure, respectively, constructed over $\mathscr{T}$. The following choices are popular.

(a) The *mini* element. This pair is studied, for instance, in [8], [21, section 4.2.4], and it is defined by

$$\mathbf{V}(\mathscr{T}) = \left\{\mathbf{v}_{\mathscr{T}}\in\mathbf{C}(\bar\Omega):\ \forall T\in\mathscr{T}, \mathbf{v}_{\mathscr{T}|T}\in[\mathbb{P}_1(T)\oplus\mathbb{B}(T)]^2\right\}\cap\mathbf{H}_0^1(\Omega), \tag{15}$$

$$\mathcal{P}(\mathscr{T}) = \left\{q_{\mathscr{T}}\in L^2(\Omega)/\mathbb{R}\cap C(\bar\Omega):\ \forall T\in\mathscr{T}, q_{\mathscr{T}|T}\in\mathbb{P}_1(T)\right\}, \tag{16}$$

where $\mathbb{B}(T)$ denotes the space spanned by a local bubble function.

(b) The Taylor–Hood pair. The lowest order Taylor–Hood element [27], [45], [21, section 4.2.5] is defined by

$$\mathbf{V}(\mathscr{T}) = \left\{\mathbf{v}_{\mathscr{T}}\in\mathbf{C}(\bar\Omega):\ \forall T\in\mathscr{T}, \mathbf{v}_{\mathscr{T}|T}\in\mathbb{P}_2(T)^2\right\}\cap\mathbf{H}_0^1(\Omega), \tag{17}$$

$$\mathcal{P}(\mathscr{T}) = \left\{q_{\mathscr{T}}\in L^2(\Omega)/\mathbb{R}\cap C(\bar\Omega):\ \forall T\in\mathscr{T}, q_{\mathscr{T}|T}\in\mathbb{P}_1(T)\right\}. \tag{18}$$

It is important to observe that if $\omega\in A_2$, we have, for the spaces defined in (15)–(18),

$$\mathbf{V}(\mathscr{T})\subset\mathbf{W}_0^{1,\infty}(\Omega)\subset\mathbf{H}_0^1(\omega,\Omega), \qquad \mathcal{P}(\mathscr{T})\subset L^\infty(\Omega)/\mathbb{R}\subset L^2(\omega,\Omega)/\mathbb{R}.$$

In addition, these spaces are compatible, in the sense that they satisfy weighted versions of the classical LBB condition [21, 24]. Namely, there exists a positive constant $\beta > 0$, which is independent of $\mathscr{T}$ and for which we have [19, Theorems 6.2 and 6.4]

$$\beta \|q_{\mathscr{T}}\|_{L^2(\mathsf{d}_z^{\pm\alpha},\Omega)} \leq \sup_{\mathbf{0}\neq \mathbf{v}_{\mathscr{T}}\in \mathbf{V}(\mathscr{T})} \frac{b_{\mp}(\mathbf{v}_{\mathscr{T}}, q_{\mathscr{T}})}{\|\nabla \mathbf{v}_{\mathscr{T}}\|_{\mathbf{L}^2(\mathsf{d}_z^{\mp\alpha},\Omega)}} \quad \forall q_{\mathscr{T}} \in \mathcal{P}(\mathscr{T}). \tag{19}$$

4.3. Finite element approximation. We now define a finite element approximation of problem (11) as follows: Find $(\mathbf{u}_{\mathscr{T}}, \mathsf{p}_{\mathscr{T}}) \in \mathbf{V}(\mathscr{T}) \times \mathcal{P}(\mathscr{T})$ such that

$$a(\mathbf{u}_{\mathscr{T}}, \mathbf{v}_{\mathscr{T}}) + b_-(\mathbf{v}_{\mathscr{T}}, \mathsf{p}_{\mathscr{T}}) + c(\mathbf{u}_{\mathscr{T}}, \mathbf{u}_{\mathscr{T}}; \mathbf{v}_{\mathscr{T}}) = \mathbf{F}\cdot \mathbf{v}_{\mathscr{T}}(z), \quad b_+(\mathbf{u}_{\mathscr{T}}, q_{\mathscr{T}}) = 0, \tag{20}$$

for all $\mathbf{v}_{\mathscr{T}} \in \mathbf{V}(\mathscr{T})$ and $q_{\mathscr{T}} \in \mathcal{P}(\mathscr{T})$.

Denote by $\mathcal{S}_{\mathscr{T}}$ the discrete version of $\mathcal{S}$. Our theory is based on the following assumption.

ASSUMPTION 4. *The operator $\mathcal{S}_{\mathscr{T}}$ is a bounded linear operator whose inverse $\mathcal{S}_{\mathscr{T}}^{-1}$ is bounded uniformly over all $\mathscr{T} \in \mathbb{T}$.*

We immediately comment that existence and uniqueness of solutions, i.e., the fact that $\mathcal{S}_{\mathscr{T}}^{-1}$ exists, is not an issue. We are in finite dimensions, and our spaces $\mathbf{V}(\mathscr{T})$ and $\mathcal{P}(\mathscr{T})$ are assumed to be compatible. The main point of the previous assumption is the existence of suitable, and uniform in $\mathbb{T}$, estimates on the solution of the discrete Stokes problem in terms of data. Under the assumption that the domain Ω is convex and the family $\mathbb{T}$ is quasi-uniform [19, Theorem 4.1] has shown that this assumption indeed holds. Whether this holds in general Lipschitz domains and in more general families of meshes is an open issue. The proof of this result is beyond the scope of our interest here.

We shall also assume, without explicitly mentioning it, that the intensity $\mathbf{F}$ of the forcing term $\mathbf{F}\delta_z$ is sufficiently small so that (12) holds with $\mathcal{S}$ replaced by $\mathcal{S}_{\mathscr{T}}$. Then, owing to [35, Corollary 4] there is a unique $(\mathbf{u}_{\mathscr{T}}, \mathsf{p}_{\mathscr{T}}) \in \mathbf{V}(\mathscr{T}) \times \mathcal{P}(\mathscr{T})$ that solves (20). Moreover, we have

$$\|\nabla \mathbf{u}_{\mathscr{T}}\|_{\mathbf{L}^2(\mathsf{d}_z^{\alpha},\Omega)} \leq \frac{3}{2} \|\mathcal{S}_{\mathscr{T}}^{-1}\| \, \|\mathbf{F}\delta_z\|_{\mathbf{H}_0^1(\mathsf{d}_z^{-\alpha},\Omega)'}, \tag{21}$$

with a pressure estimate similar to that of Proposition 3.

4.4. A quasi-interpolation operator. In order to derive reliability properties for the proposed a posteriori error estimator, it is useful to have at hand a suitable quasi-interpolation operator with optimal approximation properties [46]. We consider the operator $\Pi_{\mathscr{T}} : \mathbf{L}^1(\Omega) \to \mathbf{V}(\mathscr{T})$ analyzed in [33]. The construction of $\Pi_{\mathscr{T}}$ is inspired by the ideas developed by Clément [15], Scott and Zhang [38], and Durán and Lombardi [20]: It is built on local averages over stars and thus is well defined for functions in $\mathbf{L}^1(\Omega)$; it also exhibits optimal approximation properties. In what follows, we shall make use of the following estimates of the local interpolation error [5, 33]. To present them, we first define, for $T \in \mathscr{T}$,

$$D_T := \max_{x\in T} |x - z|. \tag{22}$$

We remind the reader that we denote by $z \in \Omega$ the support of the Dirac delta.

PROPOSITION 5 (stability and interpolation estimates). *Let $\alpha \in (-2, 2)$ and $T \in \mathscr{T}$. Then, for every $\mathbf{v} \in \mathbf{H}^1(\mathsf{d}_z^{\pm\alpha}, \mathcal{S}_T)$, we have the local stability bound*

$$\|\nabla \Pi_{\mathscr{T}} \mathbf{v}\|_{\mathbf{L}^2(\mathsf{d}_z^{\pm\alpha},T)} \lesssim \|\nabla \mathbf{v}\|_{\mathbf{L}^2(\mathsf{d}_z^{\pm\alpha},\mathcal{S}_T)} \tag{23}$$

and the interpolation error estimate

$$\|\mathbf{v}-\Pi_{\mathscr{T}}\mathbf{v}\|_{\mathbf{L}^2(\mathsf{d}_z^{\pm\alpha},T)} \lesssim h_T\|\nabla\mathbf{v}\|_{\mathbf{L}^2(\mathsf{d}_z^{\pm\alpha},\mathcal{S}_T)}. \tag{24}$$

In addition, if $\alpha\in(0,2)$*, then we have that*

$$\|\mathbf{v}-\Pi_{\mathscr{T}}\mathbf{v}\|_{\mathbf{L}^2(T)} \lesssim h_T D_T^{\frac{\alpha}{2}}\|\nabla\mathbf{v}\|_{\mathbf{L}^2(\mathsf{d}_z^{-\alpha},\mathcal{S}_T)}. \tag{25}$$

The hidden constants in the previous inequalities are independent of $\mathbf{v}$*, the cell* T*, and the mesh* $\mathscr{T}$*.*

PROPOSITION 6 (trace interpolation estimate). *Let* $\alpha\in(0,2)$*,* $T\in\mathscr{T}$*,* $S\subset\mathscr{S}_T$*, and* $\mathbf{v}\in\mathbf{H}^1(\mathsf{d}_z^{-\alpha},\mathcal{S}_T)$*. Then we have the following interpolation error estimate for the trace:*

$$\|\mathbf{v}-\Pi_{\mathscr{T}}\mathbf{v}\|_{\mathbf{L}^2(S)} \lesssim h_T^{\frac{1}{2}} D_T^{\frac{\alpha}{2}}\|\nabla\mathbf{v}\|_{\mathbf{L}^2(\mathsf{d}_z^{-\alpha},\mathcal{S}_T)}, \tag{26}$$

where the hidden constant is independent of $\mathbf{v}$*,* T*, and the mesh* $\mathscr{T}$*.*

5. A posteriori error estimates. In this section, we analyze a posteriori error estimates for the finite element approximation (20) of problem (11). To begin such an analysis, we define the velocity and pressure errors $(\boldsymbol{e}_{\mathbf{u}},e_{\mathsf{p}})$ by

$$\boldsymbol{e}_{\mathbf{u}} := \mathbf{u}-\mathbf{u}_{\mathscr{T}}\in\mathbf{H}_0^1(\mathsf{d}_z^{\alpha},\Omega),\quad e_{\mathsf{p}} := \mathsf{p}-\mathsf{p}_{\mathscr{T}}\in L^2(\mathsf{d}_z^{\alpha},\Omega)/\mathbb{R}, \tag{27}$$

respectively.

5.1. Ritz projection. In order to perform a reliability analysis for the proposed a posteriori error estimator, inspired by the developments of [3], we introduce a Ritz projection $(\boldsymbol{\Phi},\psi)$ of the residuals. The pair $(\boldsymbol{\Phi},\psi)$ is defined as the solution to the following problem: Find $(\boldsymbol{\Phi},\psi)\in\mathcal{X}$ such that

$$\begin{aligned} a(\boldsymbol{\Phi},\mathbf{v}) &= a(\boldsymbol{e}_{\mathbf{u}},\mathbf{v})+b_-(\mathbf{v},e_{\mathsf{p}})+c(\mathbf{u},\boldsymbol{e}_{\mathbf{u}};\mathbf{v})+c(\boldsymbol{e}_{\mathbf{u}},\mathbf{u}_{\mathscr{T}};\mathbf{v}),\\ (\psi,q)_{L^2(\Omega)} &= b_+(\boldsymbol{e}_{\mathbf{u}},q)\end{aligned} \tag{28}$$

for all $(\mathbf{v},q)\in\mathcal{Y}$.

The following results yields the well-posedness of problem (28).

THEOREM 7 (Ritz projection). *Problem* (28) *has a unique solution in* $\mathcal{X}$*. In addition, this solution satisfies the estimate*

$$\begin{aligned}\|\nabla\boldsymbol{\Phi}\|_{\mathbf{L}^2(\mathsf{d}_z^{\alpha},\Omega)}+\|\psi\|_{L^2(\mathsf{d}_z^{\alpha},\Omega)} &\lesssim \|\nabla\boldsymbol{e}_{\mathbf{u}}\|_{\mathbf{L}^2(\mathsf{d}_z^{\alpha},\Omega)}+\|e_{\mathsf{p}}\|_{L^2(\mathsf{d}_z^{\alpha},\Omega)}\\ &\quad+\|\nabla\boldsymbol{e}_{\mathbf{u}}\|_{\mathbf{L}^2(\mathsf{d}_z^{\alpha},\Omega)}\left(\|\nabla\mathbf{u}\|_{\mathbf{L}^2(\mathsf{d}_z^{\alpha},\Omega)}+\|\nabla\mathbf{u}_{\mathscr{T}}\|_{\mathbf{L}^2(\mathsf{d}_z^{\alpha},\Omega)}\right),\end{aligned} \tag{29}$$

where the hidden constant is independent of $(\boldsymbol{\Phi},\psi)$*,* $(\mathbf{u},\mathsf{p})$*, and* $(\mathbf{u}_{\mathscr{T}},\mathsf{p}_{\mathscr{T}})$*.*

Proof. Define

$$\mathfrak{G}:\mathbf{H}_0^1(\mathsf{d}_z^{-\alpha},\Omega)\to\mathbb{R},\quad \mathbf{v}\mapsto a(\boldsymbol{e}_{\mathbf{u}},\mathbf{v})+b_-(\mathbf{v},e_{\mathsf{p}})+c(\mathbf{u},\boldsymbol{e}_{\mathbf{u}};\mathbf{v})+c(\boldsymbol{e}_{\mathbf{u}},\mathbf{u}_{\mathscr{T}};\mathbf{v}).$$

Notice that $\mathfrak{G}$ is linear. To prove that $\mathfrak{G}\in\mathbf{H}_0^1(\mathsf{d}_z^{-\alpha},\Omega)'$, we observe that

$$\begin{aligned}|\mathfrak{G}(\mathbf{v})| \le (&\|\nabla\boldsymbol{e}_{\mathbf{u}}\|_{\mathbf{L}^2(\mathsf{d}_z^{\alpha},\Omega)}+\|e_{\mathsf{p}}\|_{L^2(\mathsf{d}_z^{\alpha},\Omega)}+\|\mathbf{u}\|_{\mathbf{L}^4(\mathsf{d}_z^{\alpha},\Omega)}\|\boldsymbol{e}_{\mathbf{u}}\|_{\mathbf{L}^4(\mathsf{d}_z^{\alpha},\Omega)}\\ &+\|\boldsymbol{e}_{\mathbf{u}}\|_{\mathbf{L}^4(\mathsf{d}_z^{\alpha},\Omega)}\|\mathbf{u}_{\mathscr{T}}\|_{\mathbf{L}^4(\mathsf{d}_z^{\alpha},\Omega)})\|\nabla\mathbf{v}\|_{\mathbf{L}^2(\mathsf{d}_z^{-\alpha},\Omega)}.\end{aligned}$$

This, combined with the Sobolev embedding $\mathbf{H}^1_0(\mathsf{d}_z^\alpha,\Omega) \hookrightarrow \mathbf{L}^4(\mathsf{d}_z^\alpha,\Omega)$ allows us to conclude.

Since $\mathsf{d}_z^\alpha \in A_2(\Omega)$ and $\mathfrak{G} \in \mathbf{H}^1_0(\mathsf{d}_z^{-\alpha},\Omega)'$, we can thus invoke the results of [34] to conclude the existence and uniqueness of $\mathbf{\Phi} \in \mathbf{H}^1_0(\mathsf{d}_z^\alpha,\Omega)$ together with the bound

$$\|\nabla \mathbf{\Phi}\|_{\mathbf{L}^2(\mathsf{d}_z^\alpha,\Omega)} \lesssim \|\nabla \boldsymbol{e}_{\mathbf{u}}\|_{\mathbf{L}^2(\mathsf{d}_z^\alpha,\Omega)} + \|e_{\mathsf{p}}\|_{L^2(\mathsf{d}_z^\alpha,\Omega)} + \|\nabla \boldsymbol{e}_{\mathbf{u}}\|_{\mathbf{L}^2(\mathsf{d}_z^\alpha,\Omega)}(\|\nabla \mathbf{u}\|_{\mathbf{L}^2(\mathsf{d}_z^\alpha,\Omega)} + \|\nabla \mathbf{u}_{\mathscr{T}}\|_{\mathbf{L}^2(\mathsf{d}_z^\alpha,\Omega)}). \tag{30}$$

On the other hand, since $\boldsymbol{e}_{\mathbf{u}} \in \mathbf{H}^1_0(\mathsf{d}_z^\alpha,\Omega)$, $b_+(\boldsymbol{e}_{\mathbf{u}},\cdot)$ defines a linear and bounded functional in $L^2(\mathsf{d}_z^{-\alpha},\Omega)/\mathbb{R}$. This immediately yields the existence and uniqueness of $\psi \in L^2(\mathsf{d}_z^\alpha,\Omega)/\mathbb{R}$ together with the estimate

$$\|\psi\|_{L^2(\mathsf{d}_z^\alpha,\Omega)} \leq \|\operatorname{div} \boldsymbol{e}_{\mathbf{u}}\|_{\mathbf{L}^2(\mathsf{d}_z^\alpha,\Omega)}.$$

A collection of the derived estimates yields (29). This concludes the proof. ∎

5.2. An upper bound for the error. With the results of Theorem 7 at hand, we observe that the pair $(\boldsymbol{e}_{\mathbf{u}}, e_{\mathsf{p}})$ satisfies the following identity:

$$a(\boldsymbol{e}_{\mathbf{u}},\mathbf{v}) + b_-(\mathbf{v},e_{\mathsf{p}}) = \mathfrak{F}(\mathbf{v}), \quad b_+(\boldsymbol{e}_{\mathbf{u}},q) = (\psi,q)_{L^2(\Omega)} \tag{31}$$

for all $(\mathbf{v},q) \in \mathcal{Y}$, where

$$\mathfrak{F} : \mathbf{H}^1_0(\mathsf{d}_z^{-\alpha},\Omega) \to \mathbb{R}, \quad \mathbf{v} \mapsto a(\mathbf{\Phi},\mathbf{v}) - c(\mathbf{u},\boldsymbol{e}_{\mathbf{u}};\mathbf{v}) - c(\boldsymbol{e}_{\mathbf{u}},\mathbf{u}_{\mathscr{T}};\mathbf{v}).$$

Thus, $(\boldsymbol{e}_{\mathbf{u}}, e_{\mathsf{p}})$ can be seen as the solution to a Stokes problem with data $(\mathfrak{F},\psi)$. It is clear that, for $\mathbf{u}$ and $\mathbf{u}_{\mathscr{T}}$ given, $\mathfrak{F}$ is linear in $\mathbf{H}^1_0(\mathsf{d}_z^{-\alpha},\Omega)$. Moreover, $\mathfrak{F} \in \mathbf{H}^1_0(\mathsf{d}_z^{-\alpha},\Omega)'$:

$$\|\mathfrak{F}\|_{\mathbf{H}^1_0(\mathsf{d}_z^{-\alpha},\Omega)'} \leq \|\nabla \mathbf{\Phi}\|_{\mathbf{L}^2(\mathsf{d}_z^\alpha,\Omega)} + C^2_{4\to 2}\|\nabla \boldsymbol{e}_{\mathbf{u}}\|_{\mathbf{L}^2(\mathsf{d}_z^\alpha,\Omega)}\left(\|\nabla \mathbf{u}\|_{\mathbf{L}^2(\mathsf{d}_z^\alpha,\Omega)} + \|\nabla \mathbf{u}_{\mathscr{T}}\|_{\mathbf{L}^2(\mathsf{d}_z^\alpha,\Omega)}\right). \tag{32}$$

With the aid of this identification, we now prove that the energy norm of the error can be bounded in terms of the energy norm of the Ritz projection, which in turn will allow us to provide computable upper bounds for the error. To do so, we must assume that the forcing term $\mathbf{F}\delta_z$ is sufficiently small so that

$$1 - \|\mathcal{S}^{-1}\| C^2_{4\to 2}\left[\|\nabla \mathbf{u}\|_{\mathbf{L}^2(\mathsf{d}_z^\alpha,\Omega)} + \|\nabla \mathbf{u}_{\mathscr{T}}\|_{\mathbf{L}^2(\mathsf{d}_z^\alpha,\Omega)}\right] \geq \lambda > 0. \tag{33}$$

Notice that if the intensity of the Dirac source $\mathbf{F}$ is such that

$$|\mathbf{F}| \leq \frac{2(1-\lambda)}{3\|\mathcal{S}^{-1}\| C^2_{4\to 2}\left(\|\mathcal{S}^{-1}\| + \|\mathcal{S}^{-1}_{\mathscr{T}}\|\right)\|\delta_z\|_{H^1_0(\mathsf{d}_z^{-\alpha},\Omega)'}},$$

then estimate (13) and its discrete analogue (21) imply condition (33).

COROLLARY 8 (upper bound for the error). *Assume that the intensity of the forcing term* $\mathbf{F}$ *is sufficiently small so that* (33) *holds. We then have that*

$$\|\nabla \boldsymbol{e}_{\mathbf{u}}\|_{\mathbf{L}^2(\mathsf{d}_z^\alpha,\Omega)} + \|e_{\mathsf{p}}\|_{L^2(\mathsf{d}_z^\alpha,\Omega)} \lesssim \|\nabla \mathbf{\Phi}\|_{\mathbf{L}^2(\mathsf{d}_z^\alpha,\Omega)} + \|\psi\|_{L^2(\mathsf{d}_z^\alpha,\Omega)}, \tag{34}$$

where the hidden constant is independent of $(\mathbf{u},\mathsf{p})$, $(\mathbf{u}_{\mathscr{T}},\mathsf{p}_{\mathscr{T}})$, *and* $(\mathbf{\Phi},\psi)$.

Proof. Since $\mathsf{d}_z^\alpha \in A_2(\Omega)$ and $\mathfrak{F} \in \mathbf{H}_0^1(\mathsf{d}_z^{-\alpha}, \Omega)'$, we can apply [34, Theorem 17] to conclude that

$$\|\nabla \boldsymbol{e}_{\mathbf{u}}\|_{\mathbf{L}^2(\mathsf{d}_z^\alpha,\Omega)} + \|e_{\mathsf{p}}\|_{L^2(\mathsf{d}_z^\alpha,\Omega)} \leq \|\mathcal{S}^{-1}\| \left(\|\nabla \boldsymbol{\Phi}\|_{\mathbf{L}^2(\mathsf{d}_z^\alpha,\Omega)} + \|\psi\|_{L^2(\mathsf{d}_z^\alpha,\Omega)} \right.$$
$$\left. + C_{4\to 2}^2 \|\nabla \boldsymbol{e}_{\mathbf{u}}\|_{\mathbf{L}^2(\mathsf{d}_z^\alpha,\Omega)} \left[\|\nabla \mathbf{u}\|_{\mathbf{L}^2(\mathsf{d}_z^\alpha,\Omega)} + \|\nabla \mathbf{u}_{\mathscr{T}}\|_{\mathbf{L}^2(\mathsf{d}_z^\alpha,\Omega)} \right] \right),$$

where we have also used estimate (32). The smallness assumption (33) allows us to absorb the last term in this estimate on the left-hand side and obtain (34). This concludes the proof. ∎

5.3. A residual-type error estimator. In this section, we propose an a posteriori error estimator for the finite element approximation (20) of problem (11).

Define, for $\alpha \in (0,2)$ and $T \in \mathscr{T}$, the *element indicator*

$$\mathscr{E}_\alpha^2(\mathbf{u}_{\mathscr{T}}, \mathsf{p}_{\mathscr{T}}; T) := h_T^2 D_T^\alpha \|\Delta \mathbf{u}_{\mathscr{T}} - (\mathbf{u}_{\mathscr{T}} \cdot \nabla)\mathbf{u}_{\mathscr{T}} - \operatorname{div} \mathbf{u}_{\mathscr{T}} \mathbf{u}_{\mathscr{T}} - \nabla \mathsf{p}_{\mathscr{T}}\|_{\mathbf{L}^2(T)}^2 \tag{35}$$
$$+ \|\operatorname{div} \mathbf{u}_{\mathscr{T}}\|_{L^2(\mathsf{d}_z^\alpha,T)}^2 + h_T D_T^\alpha \|[\![(\nabla \mathbf{u}_{\mathscr{T}} - \mathsf{p}_{\mathscr{T}} \mathbf{I}) \cdot \boldsymbol{\nu}]\!]\|_{\mathbf{L}^2(\partial T \setminus \partial\Omega)}^2 + h_T^\alpha |\mathbf{F}|^2 \#(\{z\} \cap T),$$

where $(\mathbf{u}_{\mathscr{T}}, \mathsf{p}_{\mathscr{T}})$ denotes the solution to the discrete problem (20) and $\mathbf{I} \in \mathbb{R}^{d\times d}$ denotes the identity matrix. For a set E, by $\#(E)$ we mean its cardinality. Thus $\#(\{z\} \cap T)$ equals one if $z \in T$ and zero otherwise. Here we must recall that we consider our elements T to be closed sets. For a discrete tensor valued function $\mathbf{W}_{\mathscr{T}}$, we denote by $[\![\mathbf{W}_{\mathscr{T}} \cdot \boldsymbol{\nu}]\!]$ the jump or interelement residual, which is defined, on the internal side $S \in \mathscr{S}$ shared by the distinct elements T^+, $T^- \in \mathcal{N}_S$, by

$$[\![\mathbf{W}_{\mathscr{T}} \cdot \boldsymbol{\nu}]\!] = \mathbf{W}_{\mathscr{T}}|_{T^+} \cdot \boldsymbol{\nu}^+ + \mathbf{W}_{\mathscr{T}}|_{T^-} \cdot \boldsymbol{\nu}^-. \tag{36}$$

Here $\boldsymbol{\nu}^+, \boldsymbol{\nu}^-$ are unit normals on S pointing towards T^+, T^-, respectively. The *error estimator* is thus defined as

$$\mathscr{E}_\alpha(\mathbf{u}_{\mathscr{T}}, \mathsf{p}_{\mathscr{T}}; \mathscr{T}) := \left(\sum_{T\in\mathscr{T}} \mathscr{E}_\alpha^2(\mathbf{u}_{\mathscr{T}}, \mathsf{p}_{\mathscr{T}}; T) \right)^{\frac{1}{2}}. \tag{37}$$

5.4. Reliability. We present the following global reliability result.

THEOREM 9 (global reliability). *Let $\alpha \in (0,2)$, $(\mathbf{u}, \mathsf{p}) \in \mathcal{X}$ be the solution to* (11) *and the pair $(\mathbf{u}_{\mathscr{T}}, \mathsf{p}_{\mathscr{T}}) \in (\mathbf{V}(\mathscr{T}), \mathcal{P}(\mathscr{T}))$ be its finite element approximation defined as the solution to* (20)*. Assume that the intensity of the forcing term $\mathbf{F}$ is sufficiently small so that* (33) *holds. Then*

$$\|\nabla \boldsymbol{e}_{\mathbf{u}}\|_{\mathbf{L}^2(\mathsf{d}_z^\alpha,\Omega)} + \|e_{\mathsf{p}}\|_{L^2(\mathsf{d}_z^\alpha,\Omega)} \lesssim \mathscr{E}_\alpha(\mathbf{u}_{\mathscr{T}}, \mathsf{p}_{\mathscr{T}}; \mathscr{T}), \tag{38}$$

where the hidden constant is independent of the continuous and discrete solutions, the size of the elements in the mesh $\mathscr{T}$, and $\#\mathscr{T}$, but depends on α and blows up as either $\alpha \downarrow 0$ or $\alpha \uparrow 2$.

Proof. We proceed in three steps.

Step 1. Using the first equation of (28) and (11) we obtain that

$$a(\boldsymbol{\Phi}, \mathbf{v}) = \langle \mathbf{F}\delta_z, \mathbf{v}\rangle - \sum_{T\in\mathscr{T}} \int_T (\nabla \mathbf{u}_{\mathscr{T}} : \nabla \mathbf{v} - \mathbf{u}_{\mathscr{T}} \otimes \mathbf{u}_{\mathscr{T}} : \nabla \mathbf{v} - \mathsf{p}_{\mathscr{T}} \operatorname{div} \mathbf{v}) \tag{39}$$

for every $\mathbf{v} \in \mathbf{H}^1_0(\mathtt{d}_z^{-\alpha}, \Omega)$. Integrating by parts we arrive at the identity

$$a(\mathbf{\Phi}, \mathbf{v}) = \langle \mathbf{F}\delta_z, \mathbf{v}\rangle + \sum_{S\in\mathscr{S}} \int_S [\![(\nabla \mathbf{u}_\mathscr{T} - p_\mathscr{T}\mathbf{I})\cdot\boldsymbol{\nu}]\!]\cdot\mathbf{v} + \sum_{T\in\mathscr{T}} \int_T (\Delta \mathbf{u}_\mathscr{T} - (\mathbf{u}_\mathscr{T}\cdot\nabla)\mathbf{u}_\mathscr{T} - \operatorname{div}\mathbf{u}_\mathscr{T}\mathbf{u}_\mathscr{T} - \nabla \mathtt{p}_\mathscr{T})\cdot\mathbf{v}. \tag{40}$$

Notice that to derive the previous expression, we have used that $\int_S [\![\mathbf{u}_\mathscr{T}\otimes\mathbf{u}_\mathscr{T}\cdot\boldsymbol{\nu}]\!]\cdot\mathbf{v} = 0$, which follows from the fact that our finite element velocity space consists of continuous functions.

On the other hand, the first equation of problem (20) can be rewritten as

$$\langle \mathbf{F}\delta_z, \mathbf{v}_\mathscr{T}\rangle - a(\mathbf{u}_\mathscr{T}, \mathbf{v}_\mathscr{T}) - b_-(\mathbf{v}_\mathscr{T}, \mathtt{p}_\mathscr{T}) - c(\mathbf{u}_\mathscr{T}, \mathbf{u}_\mathscr{T}; \mathbf{v}_\mathscr{T}) = 0 \quad \forall \mathbf{v}_\mathscr{T} \in \mathbf{V}(\mathscr{T}).$$

Set $\mathbf{v}_\mathscr{T} = \Pi_\mathscr{T}\mathbf{v}$ in the previous expression, apply again an integration by parts formula, and invoke (39) to arrive at the identity

$$a(\mathbf{\Phi}, \mathbf{v}) = \langle \mathbf{F}\delta_z, \mathbf{v} - \Pi_\mathscr{T}\mathbf{v}\rangle + \sum_{S\in\mathscr{S}} \int_S [\![(\nabla \mathbf{u}_\mathscr{T} - \mathtt{p}_\mathscr{T}\mathbf{I})\cdot\boldsymbol{\nu}]\!]\cdot(\mathbf{v} - \Pi_\mathscr{T}\mathbf{v}) + \sum_{T\in\mathscr{T}} \int_T (\Delta \mathbf{u}_\mathscr{T} - (\mathbf{u}_\mathscr{T}\cdot\nabla)\mathbf{u}_\mathscr{T} - \operatorname{div}\mathbf{u}_\mathscr{T}\mathbf{u}_\mathscr{T} - \nabla \mathtt{p}_\mathscr{T})\cdot(\mathbf{v} - \Pi_\mathscr{T}\mathbf{v}) = \mathbf{I} + \mathbf{II} + \mathbf{III}, \tag{41}$$

where we have also used that $\int_S [\![\mathbf{u}_\mathscr{T}\otimes\mathbf{u}_\mathscr{T}\cdot\boldsymbol{\nu}]\!]\cdot\Pi_\mathscr{T}\mathbf{v} = 0$.

We now control each term separately. To control the term $\mathbf{I}$, we first invoke the local bound of [1, Theorem 4.7] for δ_z and then the interpolation error estimate (24) and the stability bound (23) to arrive at

$$\begin{aligned}\mathbf{I} &\lesssim |\mathbf{F}|\left(h_T^{\frac{\alpha}{2}-1}\|\mathbf{v} - \Pi_\mathscr{T}\mathbf{v}\|_{\mathbf{L}^2(\mathtt{d}_z^{-\alpha},T)} + h_T^{\frac{\alpha}{2}}\|\nabla(\mathbf{v} - \Pi_\mathscr{T}\mathbf{v})\|_{\mathbf{L}^2(\mathtt{d}_z^{-\alpha},T)}\right)\\ &\lesssim |\mathbf{F}| h_T^{\frac{\alpha}{2}}\|\nabla\mathbf{v}\|_{\mathbf{L}^2(\mathtt{d}_z^{-\alpha},\mathcal{S}_T)}.\end{aligned} \tag{42}$$

The control of $\mathbf{II}$ follows from the trace interpolation error estimate (26):

$$\begin{aligned}\mathbf{II} &\lesssim \sum_{S\in\mathscr{S}} \|[\![(\nabla \mathbf{u}_\mathscr{T} - \mathtt{p}_\mathscr{T}\mathbf{I})\cdot\boldsymbol{\nu}]\!]\|_{\mathbf{L}^2(S)}\|\mathbf{v} - \Pi_\mathscr{T}\mathbf{v}\|_{\mathbf{L}^2(S)}\\ &\lesssim \sum_{S\in\mathscr{S}} h_T^{\frac{1}{2}} D_T^{\frac{\alpha}{2}}\|[\![(\nabla \mathbf{u}_\mathscr{T} - \mathtt{p}_\mathscr{T}\mathbf{I})\cdot\boldsymbol{\nu}]\!]\|_{\mathbf{L}^2(S)}\|\nabla\mathbf{v}\|_{\mathbf{L}^2(\mathtt{d}_z^{-\alpha},\mathcal{S}_T)}.\end{aligned} \tag{43}$$

We finally bound $\mathbf{III}$ using the interpolation estimate (25):

$$\mathbf{III} \lesssim \sum_{T\in\mathscr{T}} h_T D_T^{\frac{\alpha}{2}}\|\Delta \mathbf{u}_\mathscr{T} - (\mathbf{u}_\mathscr{T}\cdot\nabla)\mathbf{u}_\mathscr{T} - \operatorname{div}\mathbf{u}_\mathscr{T}\mathbf{u}_\mathscr{T} - \nabla \mathtt{p}_\mathscr{T}\|_{\mathbf{L}^2(T)}\|\nabla\mathbf{v}\|_{\mathbf{L}^2(\mathtt{d}_z^{-\alpha},\mathcal{S}_T)}. \tag{44}$$

We now apply the inf-sup condition (9), the identity (41), and the estimates obtained for the terms $\mathbf{I}$, $\mathbf{II}$, and $\mathbf{III}$ to arrive at

$$\begin{aligned}\|\nabla\mathbf{\Phi}\|^2_{\mathbf{L}^2(\mathtt{d}_z^{\alpha},\Omega)} &\lesssim \left(\sup_{\mathbf{0}\neq\mathbf{v}\in\mathbf{H}^1_0(\mathtt{d}_z^{-\alpha},\Omega)} \frac{a(\mathbf{\Phi},\mathbf{v})}{\|\mathbf{v}\|_{\mathbf{H}^1_0(\mathtt{d}_z^{-\alpha},\Omega)}}\right)^2\\ &\lesssim \sum_{T\in\mathscr{T}} \Big(h_T D_T^{\alpha}\|[\![(\nabla \mathbf{u}_\mathscr{T} - \mathtt{p}_\mathscr{T}\mathbf{I})\cdot\boldsymbol{\nu}]\!]\|^2_{\mathbf{L}^2(\partial T\setminus\partial\Omega)}\\ &\quad + h_T^2 D_T^{\alpha}\|\Delta \mathbf{u}_\mathscr{T} - (\mathbf{u}_\mathscr{T}\cdot\nabla)\mathbf{u}_\mathscr{T} - \operatorname{div}\mathbf{u}_\mathscr{T}\mathbf{u}_\mathscr{T} - \nabla \mathtt{p}_\mathscr{T}\|^2_{\mathbf{L}^2(T)} + h_T^{\alpha}|\mathbf{F}|^2\#(\{z\}\cap T)\Big),\end{aligned}$$

where, to obtain the last estimate, we have also used the finite overlapping property of stars. Notice that for $T' \in \mathcal{S}_T$, $D_{T'}$ is comparable to D_T.

Step 2. Notice that since $\psi \in L^2(\mathsf{d}_z^{\alpha}, \Omega)$, then $\tilde{q} = \mathsf{d}_z^{\alpha}\psi \in L^2(\mathsf{d}_z^{-\alpha}, \Omega)$. Define now $q = \tilde{q} + c$, where $c \in \mathbb{R}$ is chosen so that $q \in L^2(\mathsf{d}_z^{-\alpha}, \Omega)/\mathbb{R}$. This particular choice of test function for the second equation of (28) yields

$$\|\psi\|^2_{L^2(\mathsf{d}_z^{\alpha},\Omega)} = b_+(\boldsymbol{e}_{\mathbf{u}}, \mathsf{d}_z^{\alpha}\psi) = -b_+(\mathbf{u}_{\mathscr{T}}, \mathsf{d}_z^{\alpha}\psi) \leq \|\operatorname{div} \mathbf{u}_{\mathscr{T}}\|_{L^2(\mathsf{d}_z^{\alpha},\Omega)}\|\psi\|_{L^2(\mathsf{d}_z^{\alpha},\Omega)}. \tag{45}$$

Consequently, $\|\psi\|_{L^2(\mathsf{d}_z^{\alpha},\Omega)} \leq \|\operatorname{div} \mathbf{u}_{\mathscr{T}}\|_{L^2(\mathsf{d}_z^{\alpha},\Omega)}$.

Step 3. In light of the smallness assumption (33), we may apply the estimate (34) of Corollary 8 to write

$$\|\nabla \boldsymbol{e}_{\mathbf{u}}\|_{\mathbf{L}^2(\mathsf{d}_z^{\alpha},\Omega)} + \|e_{\mathsf{p}}\|_{L^2(\mathsf{d}_z^{\alpha},\Omega)} \lesssim \left(\|\nabla \boldsymbol{\Phi}\|_{\mathbf{L}^2(\mathsf{d}_z^{\alpha},\Omega)} + \|\psi\|_{L^2(\mathsf{d}_z^{\alpha},\Omega)}\right).$$

The desired estimate (38) thus follows from the estimates derived in steps 1 and 2. This concludes the proof. ∎

5.5. Local efficiency analysis. To derive efficiency properties for the local indicator $\mathscr{E}_{\alpha}(\mathbf{u}_{\mathscr{T}}, p_{\mathscr{T}}; T)$ we utilize standard residual estimation techniques but on the basis of suitable bubble functions, whose construction we owe to [1, section 5.2].

Given $T \in \mathscr{T}$, we introduce an element bubble function φ_T that satisfies $0 \leq \varphi_T \leq 1$,

$$\varphi_T(z) = 0, \qquad |T| \lesssim \int_T \varphi_T, \qquad \|\nabla \varphi_T\|_{\mathbf{L}^{\infty}(R_T)} \lesssim h_T^{-1}, \tag{46}$$

and there exists a simplex $T^* \subset T$ such that $R_T := \operatorname{supp}(\varphi_T) \subset T^*$. Notice that since φ_T satisfies (46), we have that

$$\|\theta\|_{L^2(R_T)} \lesssim \|\varphi_T^{\frac{1}{2}}\theta\|_{L^2(R_T)} \quad \forall \theta \in \mathbb{P}_5(R_T). \tag{47}$$

Given $S \in \mathscr{S}$, we introduce an edge bubble function φ_S that satisfies $0 \leq \varphi_S \leq 1$,

$$\varphi_S(z) = 0, \qquad |S| \lesssim \int_S \varphi_S, \qquad \|\nabla \varphi_S\|_{\mathbf{L}^{\infty}(R_S)} \lesssim h_S^{-1}, \tag{48}$$

and $R_S := \operatorname{supp}(\varphi_S)$ is such that if $\mathcal{N}_S = \{T, T'\}$, there are simplices $T_* \subset T$ and $T'_* \subset T'$ such that $R_S \subset T_* \cup T'_* \subset T \cup T'$.

PROPOSITION 10 (estimates for bubble functions). *Let $T \in \mathscr{T}$ and φ_T be the bubble function that satisfies* (46)*. If $\alpha \in (0, 2)$, then*

$$h_T\|\nabla(\theta\varphi_T)\|_{\mathbf{L}^2(\mathsf{d}_z^{-\alpha},T)} \lesssim D_T^{-\frac{\alpha}{2}}\|\theta\|_{L^2(T)} \quad \forall \theta \in \mathbb{P}_5(T). \tag{49}$$

Let $S \in \mathscr{S}$ and φ_S be the bubble function that satisfies (48)*. If $\alpha \in (0, 2)$, then*

$$h_T^{\frac{1}{2}}\|\nabla(\theta\varphi_S)\|_{\mathbf{L}^2(\mathsf{d}_z^{-\alpha},\mathcal{N}_S)} \lesssim D_T^{-\frac{\alpha}{2}}\|\theta\|_{L^2(S)} \quad \forall \theta \in \mathbb{P}_3(S), \tag{50}$$

where θ is extended to the elements that comprise $\mathcal{N}_S$ as a constant along the direction normal to S.

Proof. See [1, Lemma 5.2]. ∎

Having constructed these local bubble functions, the local efficiency can be shown following more or less standard arguments.

THEOREM 11 (local efficiency). *Let $\alpha \in (0,2)$, let $(\mathbf{u},\mathsf{p}) \in \mathcal{X}$ be the solution to problem* (11)*, and let $(\mathbf{u}_{\mathscr{T}},\mathsf{p}_{\mathscr{T}}) \in \mathbf{V}(\mathscr{T}) \times \mathcal{P}(\mathscr{T})$ be its finite element approximation given as the solution to* (20)*. Assume that the intensity of the forcing term $\mathbf{F}$ is sufficiently small so that* (33) *holds. Then*

$$\mathscr{E}_\alpha^2(\mathbf{u}_{\mathscr{T}},\mathsf{p}_{\mathscr{T}};T) \lesssim \|\nabla \mathbf{e}_{\mathbf{u}}\|^2_{\mathbf{L}^2(\mathsf{d}_z^\alpha,\mathcal{N}_T)} + \|e_{\mathsf{p}}\|^2_{L^2(\mathsf{d}_z^\alpha,\mathcal{N}_T)}, \tag{51}$$

where the hidden constant is independent of the continuous and discrete solutions, the size of the elements in the mesh $\mathscr{T}$, and $\#\mathscr{T}$, but depends on α and blows up as either $\alpha \downarrow 0$ or $\alpha \uparrow 2$.

Proof. We estimate each contribution in (35) separately, so the proof has several steps.

Step 1. For $T \in \mathscr{T}$ we bound the bulk term $h_T^2 D_T^\alpha \|\Delta \mathbf{u}_{\mathscr{T}} - (\mathbf{u}_{\mathscr{T}}\cdot\nabla)\mathbf{u}_{\mathscr{T}} - \operatorname{div}\mathbf{u}_{\mathscr{T}}\mathbf{u}_{\mathscr{T}} - \nabla p_{\mathscr{T}}\|^2_{\mathbf{L}^2(T)}$. To shorten notation, we define the functions

$$\mathbf{X}_T := (\Delta \mathbf{u}_{\mathscr{T}} - (\mathbf{u}_{\mathscr{T}}\cdot\nabla)\mathbf{u}_{\mathscr{T}} - \operatorname{div}\mathbf{u}_{\mathscr{T}}\mathbf{u}_{\mathscr{T}} - \nabla p_{\mathscr{T}})_{|T}, \quad \boldsymbol{\Upsilon}_T := \varphi_T \mathbf{X}_T.$$

Since $\varphi_T(z) = 0$, we immediately conclude that $\boldsymbol{\Upsilon}_T(z) = \varphi_T(z)\mathbf{X}_T(z) = \mathbf{0}$. We utilize the definitions of $\mathbf{X}_T$ and $\boldsymbol{\Upsilon}_T$ and invoke (47) to conclude that

$$\begin{aligned}\|\Delta \mathbf{u}_{\mathscr{T}} - (\mathbf{u}_{\mathscr{T}}\cdot\nabla)\mathbf{u}_{\mathscr{T}} - \operatorname{div}\mathbf{u}_{\mathscr{T}}\mathbf{u}_{\mathscr{T}} - \nabla p_{\mathscr{T}}\|^2_{\mathbf{L}^2(T)} \\ \lesssim \int_{R_T} |\mathbf{X}_T|^2 \varphi_T = \int_T \mathbf{X}_T \cdot \boldsymbol{\Upsilon}_T.\end{aligned} \tag{52}$$

Set $\mathbf{v} = \boldsymbol{\Upsilon}_T$ as test function in identity (40), and use that $\boldsymbol{\Upsilon}_T(z) = 0$ and that $\boldsymbol{\Upsilon}_{T|S} = \mathbf{0}$, for $S \in \mathscr{S}_T$, to arrive at

$$\int_T \mathbf{X}_T \cdot \boldsymbol{\Upsilon}_T = a(\boldsymbol{\Phi}, \boldsymbol{\Upsilon}_T).$$

Since $\operatorname{supp}\boldsymbol{\Upsilon}_T \subset T$, a local version of the argument that led to estimate (29) implies that

$$\begin{aligned}a(\boldsymbol{\Phi}, \boldsymbol{\Upsilon}_T) \lesssim \big(\|\nabla \boldsymbol{e}_{\mathbf{u}}\|_{\mathbf{L}^2(\mathsf{d}_z^\alpha,T)} + \|e_{\mathsf{p}}\|_{L^2(\mathsf{d}_z^\alpha,T)} + \|\nabla \mathbf{u}\|_{\mathbf{L}^2(\mathsf{d}_z^\alpha,T)}\|\nabla \boldsymbol{e}_{\mathbf{u}}\|_{\mathbf{L}^2(\mathsf{d}_z^\alpha,T)} \\ + \|\nabla \boldsymbol{e}_{\mathbf{u}}\|_{\mathbf{L}^2(\mathsf{d}_z^\alpha,T)}\|\nabla \mathbf{u}_{\mathscr{T}}\|_{\mathbf{L}^2(\mathsf{d}_z^\alpha,T)}\big)\|\nabla \boldsymbol{\Upsilon}_T\|_{\mathbf{L}^2(\mathsf{d}_z^{-\alpha},T)}.\end{aligned}$$

Next, we utilize the smallness assumption (33), which implies the estimate

$$\|\nabla \mathbf{u}\|_{\mathbf{L}^2(\mathsf{d}_z^\alpha,\Omega)} + \|\nabla \mathbf{u}_{\mathscr{T}}\|_{\mathbf{L}^2(\mathsf{d}_z^\alpha,\Omega)} \leq \frac{1-\lambda}{\|\mathcal{S}^{-1}\| C_{4\to 2}^2},$$

to obtain that

$$a(\boldsymbol{\Phi}, \boldsymbol{\Upsilon}_T) \lesssim \big(\|\nabla \boldsymbol{e}_{\mathbf{u}}\|_{\mathbf{L}^2(\mathsf{d}_z^\alpha,T)} + \|e_{\mathsf{p}}\|_{L^2(\mathsf{d}_z^\alpha,T)}\big)\|\nabla \boldsymbol{\Upsilon}_T\|_{\mathbf{L}^2(\mathsf{d}_z^{-\alpha},T)}. \tag{53}$$

We thus substitute this estimate in (52) to derive

$$\|\mathbf{X}_T\|^2_{\mathbf{L}^2(T)} \lesssim \big(\|\nabla \boldsymbol{e}_{\mathbf{u}}\|_{\mathbf{L}^2(\mathsf{d}_z^\alpha,T)} + \|e_{\mathsf{p}}\|_{L^2(\mathsf{d}_z^\alpha,T)}\big)\|\nabla \boldsymbol{\Upsilon}_T\|_{\mathbf{L}^2(\mathsf{d}_z^{-\alpha},T)}. \tag{54}$$

We now recall that $\boldsymbol{\Upsilon}_T := \varphi_T \mathbf{X}_T$ and invoke estimate (49) to arrive at

$$\|\nabla \boldsymbol{\Upsilon}_T\|_{\mathbf{L}^2(\mathsf{d}_z^{-\alpha},T)} \lesssim h_T^{-1} D_T^{-\alpha/2} \|\mathbf{X}_T\|_{\mathbf{L}^2(T)}.$$

The previous two estimates yield the desired bound on the first term:

$$h_T^2 D_T^\alpha \|\Delta \mathbf{u}_{\mathscr{T}} - (\mathbf{u}_{\mathscr{T}} \cdot \nabla)\mathbf{u}_{\mathscr{T}} - \operatorname{div} \mathbf{u}_{\mathscr{T}}\mathbf{u}_{\mathscr{T}} - \nabla \mathsf{p}_{\mathscr{T}}\|^2_{\mathbf{L}^2(T)} \lesssim \|\nabla \boldsymbol{e}_{\mathbf{u}}\|^2_{\mathbf{L}^2(\mathsf{d}_z^\alpha, T)} + \|e_{\mathsf{p}}\|^2_{L^2(\mathsf{d}_z^\alpha, T)}. \tag{55}$$

Step 2. In this step we control the jump term $h_T D_T^\alpha \|[\![(\nabla \mathbf{u}_{\mathscr{T}} - \mathsf{p}_{\mathscr{T}}\mathbf{I})\cdot \boldsymbol{\nu}]\!]\|^2_{\mathbf{L}^2(S)}$. Let $T \in \mathscr{T}$ and $S \in \mathscr{S}_T$. Define $\boldsymbol{\Lambda}_S = \varphi_S [\![(\nabla \mathbf{u}_{\mathscr{T}} - \mathsf{p}_{\mathscr{T}}\mathbf{I})\cdot \boldsymbol{\nu}]\!]$ so that, using (48), we have

$$\begin{aligned} \|[\![(\nabla \mathbf{u}_{\mathscr{T}} - \mathsf{p}_{\mathscr{T}}\mathbf{I})\cdot \boldsymbol{\nu}]\!]\|^2_{\mathbf{L}^2(S)} &\lesssim \int_S |[\![(\nabla \mathbf{u}_{\mathscr{T}} - \mathsf{p}_{\mathscr{T}}\mathbf{I})\cdot \boldsymbol{\nu}]\!]|^2 \varphi_S \\ &= \int_S [\![(\nabla \mathbf{u}_{\mathscr{T}} - \mathsf{p}_{\mathscr{T}}\mathbf{I})\cdot \boldsymbol{\nu}]\!]\cdot \boldsymbol{\Lambda}_S. \end{aligned} \tag{56}$$

Setting $\mathbf{v} = \boldsymbol{\Lambda}_S$ in (40) and using that $\boldsymbol{\Lambda}_S(z) = \mathbf{0}$ yields

$$\int_S [\![(\nabla \mathbf{u}_{\mathscr{T}} - \mathsf{p}_{\mathscr{T}}\mathbf{I})\cdot \boldsymbol{\nu}]\!]\cdot \boldsymbol{\Lambda}_S = a(\boldsymbol{\Phi}, \boldsymbol{\Lambda}_S) - \sum_{T' \in \mathcal{N}_S} \int_{T'} \mathbf{X}_{T'} \cdot \boldsymbol{\Lambda}_S.$$

Now, since $\operatorname{supp}(\boldsymbol{\Lambda}_S) \subseteq R_S = \operatorname{supp}(\varphi_S) \subset T_* \cup T_*' \subset \cup\{T' : T' \in \mathcal{N}_S\}$, arguments similar to those that led to (53) allow us to obtain

$$\begin{aligned} &\int_S [\![(\nabla \mathbf{u}_{\mathscr{T}} - \mathsf{p}_{\mathscr{T}}\mathbf{I})\cdot \boldsymbol{\nu}]\!]\cdot \boldsymbol{\Lambda}_S \\ &\qquad \le |a(\boldsymbol{\Phi}, \boldsymbol{\Lambda}_S)| + \sum_{T' \in \mathcal{N}_S} \|\mathbf{X}_{T'}\|_{\mathbf{L}^2(T')} \|\boldsymbol{\Lambda}_S\|_{\mathbf{L}^2(T')} \\ &\qquad \lesssim \sum_{T' \in \mathcal{N}_S} \left(\|\nabla \boldsymbol{e}_{\mathbf{u}}\|_{\mathbf{L}^2(\mathsf{d}_z^\alpha, T')} + \|e_{\mathsf{p}}\|_{L^2(\mathsf{d}_z^\alpha, T')}\right) \|\nabla \boldsymbol{\Lambda}_S\|_{\mathbf{L}^2(\mathsf{d}_z^{-\alpha}, T')} \\ &\qquad\qquad + \sum_{T' \in \mathcal{N}_S} \|\mathbf{X}_{T'}\|_{\mathbf{L}^2(T')} \|\boldsymbol{\Lambda}_S\|_{\mathbf{L}^2(T')}. \end{aligned}$$

By shape regularity we have that $|T'| \approx h_{T'}^2$ and $|S| \approx h_{T'}$. Moreover, since the function $\boldsymbol{\Lambda}_S$ is the product of a fixed, and smooth, function by a polynomial, equivalence of norms, scaling arguments, and the previous two observations yield

$$\|\boldsymbol{\Lambda}_S\|_{\mathbf{L}^2(T')} \approx |T'|^{\frac{1}{2}} |S|^{-\frac{1}{2}} \|\boldsymbol{\Lambda}_S\|_{\mathbf{L}^2(S)} \approx h_{T'}^{\frac{1}{2}} \|\boldsymbol{\Lambda}_S\|_{\mathbf{L}^2(S)},$$

where the hidden constants depend only on the polynomial degree. This, estimate (50), and the bound on $\mathbf{X}_{T'}$ derived in (55) yield

$$\begin{aligned} &\int_S [\![(\nabla \mathbf{u}_{\mathscr{T}} - \mathsf{p}_{\mathscr{T}}\mathbf{I})\cdot \boldsymbol{\nu}]\!]\cdot \boldsymbol{\Lambda}_S \\ &\qquad \lesssim \sum_{T' \in \mathcal{N}_S} \left(\|\nabla \boldsymbol{e}_{\mathbf{u}}\|_{\mathbf{L}^2(\mathsf{d}_z^\alpha, T')} + \|e_{\mathsf{p}}\|_{L^2(\mathsf{d}_z^\alpha, T')}\right) h_T^{-\frac{1}{2}} D_T^{-\frac{\alpha}{2}} \|\boldsymbol{\Lambda}_S\|_{\mathbf{L}^2(S)}. \end{aligned}$$

We replace the previous estimate in (56) to arrive at

$$h_T D_T^\alpha \|[\![(\nabla \mathbf{u}_{\mathscr{T}} - p_{\mathscr{T}}\mathbf{I})\cdot \boldsymbol{\nu}]\!]\|^2_{\mathbf{L}^2(S)} \lesssim \sum_{T' \in \mathcal{N}_S} \left(\|\nabla \boldsymbol{e}_{\mathbf{u}}\|^2_{\mathbf{L}^2(\mathsf{d}_z^\alpha, T')} + \|e_{\mathsf{p}}\|^2_{L^2(\mathsf{d}_z^\alpha, T')}\right). \tag{57}$$

Since every $T \in \mathscr{T}$ belongs to at most three sets in the collection $\{\mathcal{N}_S : S \in \mathscr{S}\}$, we can conclude.

Step 3. We now bound the residual term associated with the incompressibility constraint. Since $\operatorname{div} \mathbf{u} = 0$, for any $T \in \mathscr{T}$, we immediately arrive at

$$\| \operatorname{div} \mathbf{u}_{\mathscr{T}} \|_{L^2(\mathsf{d}_z^\alpha,T)} = \| \operatorname{div} \boldsymbol{e}_{\mathbf{u}} \|_{L^2(\mathsf{d}_z^\alpha,T)} \lesssim \|\nabla \boldsymbol{e}_{\mathbf{u}}\|_{\mathbf{L}^2(\mathsf{d}_z^\alpha,T)}. \tag{58}$$

Step 4. We now bound the term associated with the singular source. Let $T \in \mathscr{T}$ and note that if $T \cap \{z\} = \emptyset$, then there is nothing to prove. Otherwise, we must obtain a bound for the term $h_T^\alpha |\mathbf{F}|^2$. To do so we follow the arguments developed in the proof of [1, Theorem 5.3] that yield the existence of a smooth function η such that

$$\eta(z) = 1, \quad \|\eta\|_{L^\infty(\Omega)} = 1, \quad \|\nabla \eta\|_{\mathbf{L}^\infty(\Omega)} \lesssim h_T^{-1}, \quad \operatorname{supp}(\eta) \subset \mathcal{N}_T. \tag{59}$$

Define $\mathbf{v}_\eta := \mathbf{F}\eta \in \mathbf{H}^1_0(\mathsf{d}_z^{-\alpha}, \Omega)$. Since $(\mathbf{u}, \mathsf{p})$ and $(\boldsymbol{\Phi}, \psi)$ solve (11) and (28), respectively, we obtain

$$\begin{aligned} |\mathbf{F}|^2 = \langle \mathbf{F}\delta_z, \mathbf{v}_\eta \rangle &= a(\mathbf{u}, \mathbf{v}_\eta) + b_-(\mathbf{v}_\eta, \mathsf{p}) + c(\mathbf{u}, \mathbf{u}; \mathbf{v}_\eta) \\ &= a(\boldsymbol{\Phi}, \mathbf{v}_\eta) + a(\mathbf{u}_{\mathscr{T}}, \mathbf{v}_\eta) + b_-(\mathbf{v}_\eta, \mathsf{p}_{\mathscr{T}}) + c(\mathbf{u}_{\mathscr{T}}, \mathbf{u}_{\mathscr{T}}; \mathbf{v}_\eta). \end{aligned}$$

Since $\operatorname{supp}(\eta) \subset \mathcal{N}_T$, we apply arguments similar to those that led to (53), integration by parts, and basic estimates to arrive at

$$\begin{aligned} |\mathbf{F}|^2 \lesssim{}& \left(\|\nabla \mathbf{e}_{\mathbf{u}}\|_{\mathbf{L}^2(\mathsf{d}_z^\alpha, \mathcal{N}_T)} + \|e_{\mathsf{p}}\|_{L^2(\mathsf{d}_z^\alpha, \mathcal{N}_T)} \right) \|\nabla \mathbf{v}_\eta\|_{\mathbf{L}^2(\mathsf{d}_z^{-\alpha}, \mathcal{N}_T)} \\ &+ \sum_{T' \in \mathscr{T} : T' \subset \mathcal{N}_T} \|\Delta \mathbf{u}_{\mathscr{T}} - (\mathbf{u}_{\mathscr{T}} \cdot \nabla)\mathbf{u}_{\mathscr{T}} - \operatorname{div} \mathbf{u}_{\mathscr{T}} \mathbf{u}_{\mathscr{T}} - \nabla \mathsf{p}_{\mathscr{T}}\|_{\mathbf{L}^2(T')} \|\mathbf{v}_\eta\|_{\mathbf{L}^2(T')} \\ &+ \sum_{T' \in \mathscr{T} : T' \subset \mathcal{N}_T} \sum_{S \in \mathscr{S}_{T'} : S \not\subset \partial \mathcal{N}_T} \|[\![(\nabla \mathbf{u}_{\mathscr{T}} - \mathsf{p}_{\mathscr{T}} \mathbf{I}) \cdot \boldsymbol{\nu}]\!]\|_{\mathbf{L}^2(S)} \|\mathbf{v}_\eta\|_{\mathbf{L}^2(S)}. \end{aligned}$$

We now use the estimates

$$\|\eta\|_{L^2(S)} \lesssim h_T^{\frac{1}{2}}, \quad \|\eta\|_{L^2(\mathcal{N}_T)} \lesssim h_T, \quad \|\nabla \eta\|_{\mathbf{L}^2(\mathsf{d}_z^{-\alpha}, \mathcal{N}_T)} \lesssim h_T^{-\frac{\alpha}{2}},$$

and the fact that since $z \in T$, we have $h_T \approx D_T$, to assert the bound

$$\begin{aligned} |\mathbf{F}|^2 \lesssim{}& h_T^{-\frac{\alpha}{2}} |\mathbf{F}| \left(\|\nabla \mathbf{e}_{\mathbf{u}}\|^2_{\mathbf{L}^2(\mathsf{d}_z^\alpha, \mathcal{N}_T)} + \|e_{\mathsf{p}}\|^2_{L^2(\mathsf{d}_z^\alpha, \mathcal{N}_T)} \right)^{\frac{1}{2}} \\ &+ h_T^{-\frac{\alpha}{2}} |\mathbf{F}| \Bigg(\sum_{T' \in \mathscr{T} : T' \subset \mathcal{N}_T} h_{T'} D_{T'}^{\frac{\alpha}{2}} \|\Delta \mathbf{u}_{\mathscr{T}} - (\mathbf{u}_{\mathscr{T}} \cdot \nabla)\mathbf{u}_{\mathscr{T}} - \operatorname{div} \mathbf{u}_{\mathscr{T}} \mathbf{u}_{\mathscr{T}} - \nabla \mathsf{p}_{\mathscr{T}}\|_{\mathbf{L}^2(T')} \\ &\qquad + \sum_{T' \in \mathscr{T} : T' \subset \mathcal{N}_{T'}} \sum_{S \in \mathscr{S}_{T'} : S \not\subset \partial \mathcal{N}_T} D_{T'}^{\frac{\alpha}{2}} h_{T'}^{\frac{1}{2}} \|[\![(\nabla \mathbf{u}_{\mathscr{T}} - \mathsf{p}_{\mathscr{T}} \mathbf{I}) \cdot \boldsymbol{\nu}]\!]\|_{\mathbf{L}^2(S)} \Bigg). \end{aligned} \tag{60}$$

Invoke (55) and (57) to conclude.

Step 5. Collect the estimates derived in the previous steps to arrive at the desired local efficiency estimate (51). ∎

6. Numerical results. In this section we present a series of numerical examples that illustrate the performance of the devised error estimator $\mathscr{E}_\alpha(\mathbf{u}_{\mathscr{T}}, \mathsf{p}_{\mathscr{T}}; \mathscr{T})$ defined in (37). In some of these examples, we go beyond the presented theory and perform numerical experiments where we violate the assumption of homogeneous Dirichlet boundary conditions. The examples have been carried out with the help of a

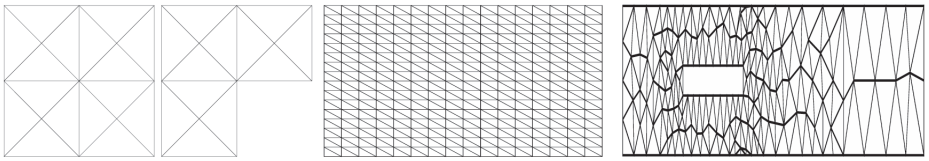

FIG. 1. *The initial meshes $\mathscr{T}_0$ used in the adaptive algorithm, Algorithm* 1*, when* (a) $\Omega = (0,1)^2$, (b) $\Omega = (-1,1)^2 \setminus [0,1) \times [-1,0)$, (c) $\Omega = (0,4) \times (0,1)$, *and* (d) $\Omega = (0,10) \times (0,1) \setminus [2,4] \times [0.4, 0.6]$.

code that we implemented using `C++`. All matrices have been assembled exactly, and global linear systems were solved using the multifrontal massively parallel sparse direct solver (MUMPS) [6, 7]. The right-hand sides, the terms involving the weight, and the approximation errors are computed by a quadrature formula which is exact for polynomials of degree 19.

For a given partition $\mathscr{T}$, we solve the discrete problem (20) with the discrete spaces (17)–(18). This setting will be referred to as Taylor–Hood approximation. To obtain the solution of (20) we use a fixed–point strategy, which is described in Algorithm 2. In this algorithm, the initial guess is obtained as a discrete approximation of the solution to a Stokes problem with singular sources [5] and tol $= 10^{-8}$. Once the discrete solution $(\mathbf{u}_{\mathscr{T}}, \mathsf{p}_{\mathscr{T}})$ is obtained, we compute, for $T \in \mathscr{T}$, the a posteriori error indicators $\mathscr{E}_\alpha(\mathbf{u}_{\mathscr{T}}, \mathsf{p}_{\mathscr{T}}; T)$, given in (35), to drive the adaptive mesh refinement procedure described in Algorithm 1. Every mesh $\mathscr{T}$ is adaptively refined by marking for refinement the elements $T \in \mathscr{T}$ that are such that step 3 in Algorithm 1 holds. A sequence of adaptively refined meshes is thus generated from the initial meshes shown in Figure 1.

We define the total number of degrees of freedom as $\mathsf{Ndof} := \dim \mathbf{V}(\mathscr{T}) + \dim \mathcal{P}(\mathscr{T})$. We recall that the discrete spaces $\mathbf{V}(\mathscr{T})$ and $\mathcal{P}(\mathscr{T})$ are as in (17) and (18), respectively.

Algorithm 1 Adaptive Algorithm.

Input: Initial mesh $\mathscr{T}_0$, interior point $z \in \Omega$, and $\alpha \in (0,2)$;
1: Solve the discrete problem (20) by using Algorithm 2;
2: For each $T \in \mathscr{T}$ compute the local error indicators $\mathscr{E}_\alpha(\mathbf{u}_{\mathscr{T}}, p_{\mathscr{T}}; T)$ given in (35);
3: Mark an element $T \in \mathscr{T}$ for refinement if

$$\mathscr{E}_\alpha(\mathbf{u}_{\mathscr{T}}, p_{\mathscr{T}}; T) > \frac{1}{2} \max_{T' \in \mathscr{T}} \mathscr{E}_\alpha(\mathbf{u}_{\mathscr{T}}, p_{\mathscr{T}}; T');$$

4: From step **3**, construct a new mesh, using a longest edge bisection algorithm [29]. Set $i \leftarrow i + 1$, and go to step **1**.

6.1. Convex and nonconvex domains with homogeneous boundary conditions. We first explore the performance of the devised a posteriori error estimator in problems with homogeneous boundary conditions on convex and nonconvex domains Ω.

6.1.1. Convex domain. We set $\Omega = (0,1)^2$, $z = (0.5, 0.5)^\intercal$, and $\mathbf{F} = (1,1)^\intercal$. We explore the performance of $\mathscr{E}_\alpha$ when driving the adaptive procedure of Algorithm 1. We also investigate the effect of varying the exponent α in the Muckenhoupt weight. To accomplish this task, we consider $\alpha \in \{0.25, 0.5, 0.75, 1.0, 1.25, 1.5, 1.75\}$.

Algorithm 2 Fixed-Point Algorithm.

Input: Initial guess $(\mathbf{u}^0_{\mathscr{T}}, \mathsf{p}^0_{\mathscr{T}}) \in \mathbf{V}(\mathscr{T}) \times \mathcal{P}(\mathscr{T})$ and tol. Set $i = 1$;
1: Find $(\mathbf{u}^i_{\mathscr{T}}, p^i_{\mathscr{T}}) \in \mathbf{V}(\mathscr{T}) \times \mathcal{P}(\mathscr{T})$ such that

$$a(\mathbf{u}^i_{\mathscr{T}}, \mathbf{v}_{\mathscr{T}}) + b_-(\mathbf{v}_{\mathscr{T}}, \mathsf{p}^i_{\mathscr{T}}) + c(\mathbf{u}^{i-1}_{\mathscr{T}}, \mathbf{u}^i_{\mathscr{T}}; \mathbf{v}_{\mathscr{T}}) = \mathbf{F} \cdot \mathbf{v}_{\mathscr{T}}(z), \quad b_+(\mathbf{u}^i_{\mathscr{T}}, q_{\mathscr{T}}) = 0,$$

for all $(\mathbf{v}_{\mathscr{T}}, q_{\mathscr{T}}) \in \mathbf{V}(\mathscr{T}) \times \mathcal{P}(\mathscr{T})$;
2: If $|(\mathbf{u}^i_{\mathscr{T}}, p^i_{\mathscr{T}}) - (\mathbf{u}^{i-1}_{\mathscr{T}}, p^{i-1}_{\mathscr{T}})| >$ tol, set $i \leftarrow i + 1$, and go to step **1**. Otherwise, **return** $(\mathbf{u}_{\mathscr{T}}, \mathsf{p}_{\mathscr{T}}) = (\mathbf{u}^i_{\mathscr{T}}, \mathsf{p}^i_{\mathscr{T}})$.

In Figure 2 we present the experimental rates of convergence for the error estimator $\mathscr{E}_\alpha$. We also present the meshes obtained after 20 adaptive refinements for $\alpha \in \{0.25, 1.0, 1.5\}$. We observe that optimal experimental rates of convergence are attained for all the values of the parameter α that we considered. We also observe that most of the refinement is concentrated around the singular source point. In Figure 3 we present effectivity indices $\mathsf{Eff}_{\mathsf{R}}(\alpha)$ for $\alpha \in \{0.5, 1.0, 1.5\}$. Since no exact solution is available, we consider as an exact solution a discrete one, which we denote by $(\mathbf{u}_{\mathscr{T}_R}, p_{\mathscr{T}_R})$ and is obtained after performing enough adaptive refinements in order to surpass one million degrees of freedom. The effectivity indices are calculated as follows:

$$\mathsf{Eff}_{\mathsf{R}}(\alpha) = \frac{\mathscr{E}_\alpha(\mathbf{u}_{\mathscr{T}}, \mathsf{p}_{\mathscr{T}}; \mathscr{T})}{\|\nabla(\mathbf{u}_{\mathscr{T}_R} - \mathbf{u}_{\mathscr{T}})\|_{\mathbf{L}^2(\mathsf{d}_z^\alpha, \Omega)} + \|p_{\mathscr{T}_R} - p_{\mathscr{T}}\|_{L^2(\mathsf{d}_z^\alpha, \Omega)}}. \tag{61}$$

From Figure 3 it can be observed that, for all the values of the parameter α that we consider, the effectivity indices are stabilized around the value of 6. This shows the accuracy of the proposed error estimator when it is used in our adaptive algorithm.

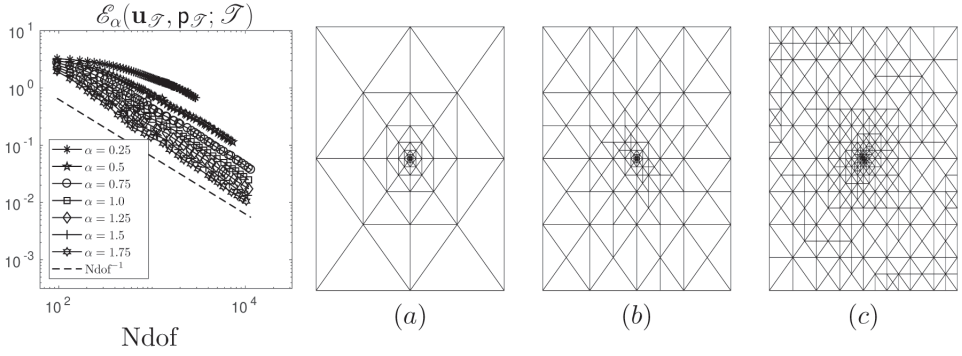

FIG. 2. Convex domain: *Experimental rates of convergence for the error estimator* $\mathscr{E}_\alpha(\mathbf{u}_{\mathscr{T}}, \mathsf{p}_{\mathscr{T}}; \mathscr{T})$ *considering* $\alpha \in \{0.25, 0.5, 0.75, 1.0, 1.25, 1.5, 1.75\}$ *(left) and the meshes obtained after* 20 *adaptive refinements for* (a) $\alpha = 0.25$ *(*168 *elements and* 89 *vertices);* (b) $\alpha = 1.0$ *(*252 *elements and* 137 *vertices); and* (c) $\alpha = 1.75$ *(*664 *elements and* 355 *vertices).*

6.1.2. Nonconvex domain. We set $\Omega = (-1, 1)^2 \setminus [0, 1) \times [-1, 0)$, an L-shaped domain, $z = (0.5, 0.5)^\intercal$, and $\mathbf{F} = (1, 1)^\intercal$. We again consider different values of the exponent α of the Muckenhoupt weight d_z^α defined in (3). We consider $\alpha \in \{0.25, 0.5, 0.75, 1.0, 1.25, 1.5, 1.75\}$.

In Figure 4 we present the experimental rates of convergence for the error estimator $\mathscr{E}_\alpha$. We also present the meshes obtained after 25 adaptive refinements for

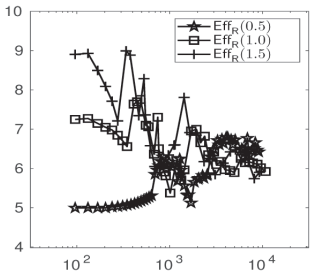

FIG. 3. Convex domain: *Effectivity indices* $\mathsf{Eff}_R(\alpha)$*, which are calculated as in* (61)*, for* $\alpha \in \{0.5, 1.0, 1.5\}$.

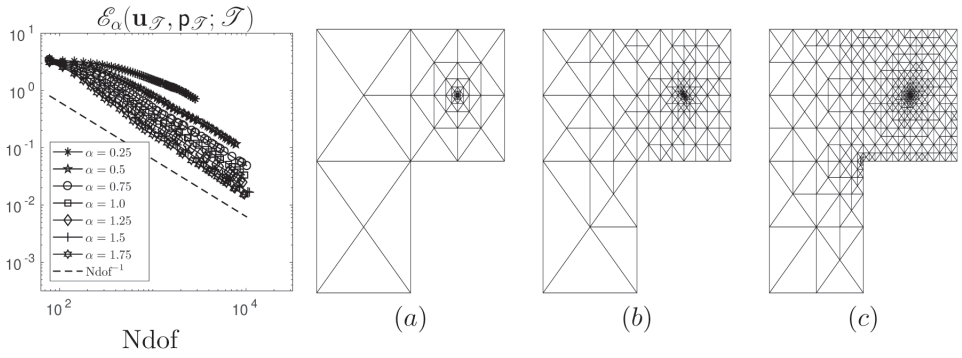

FIG. 4. Nonconvex domain: *Experimental rates of convergence for the error estimator* $\mathscr{E}_\alpha(\mathbf{u}_\mathscr{T}, \mathsf{p}_\mathscr{T}; \mathscr{T})$ *considering* $\alpha \in \{0.25, 0.5, 0.75, 1.0, 1.25, 1.5, 1.75\}$ *(left) and the meshes obtained after* 25 *adaptive refinements for* (a) $\alpha = 0.25$ *(*201 *elements and* 107 *vertices);* (b) $\alpha = 1.0$ *(*412 *elements and* 222 *vertices); and* (c) $\alpha = 1.75$ *(*923 *elements and* 493 *vertices).*

$\alpha \in \{0.25, 1.0, 1.5\}$. We observe that for all the values of the parameter α that we have considered, optimal experimental rates of convergence are attained. We also observe that most of the refinement is concentrated around the singular source point and that the geometric singularity is rapidly noticed for values of α closer to two.

6.2. A series of Dirac sources. We now go beyond the presented theory and include a series of Dirac delta sources on the right-hand side of the momentum equation. To be precise, we will replace the momentum equation in (1) by

$$-\Delta \mathbf{u} + (\mathbf{u}\cdot\nabla)\mathbf{u} + \nabla \mathsf{p} = \sum_{z\in\mathcal{Z}} \mathbf{F}_z \delta_z \text{ in } \Omega, \tag{62}$$

where $\mathcal{Z} \subset \Omega$ denotes a finite set with cardinality $\#\mathcal{Z}$ which is such that $1 < \#\mathcal{Z}$ and $\{\mathbf{F}_z\}_{z\in\mathcal{Z}} \subset \mathbb{R}^2$. We introduce the weight [4, section 5]

$$\rho(x) = \begin{cases} \mathsf{d}_z^\alpha, & \exists\, z \in \mathcal{Z} : |x - z| < \frac{d_\mathcal{Z}}{2}, \\ 1, & |x - z| \geq \frac{d_\mathcal{Z}}{2} \ \forall\, z \in \mathcal{Z}, \end{cases} \tag{63}$$

where $d_\mathcal{Z} = \min\{\mathsf{dist}(\mathcal{Z}, \partial\Omega), \min\{|z - z'| : z, z' \in \mathcal{Z}, z \neq z'\}\}$. This weight belongs to the Muckenhoupt class A_2 [2] and to the restricted class $A_2(\Omega)$. With the weight ρ at hand, we modify the definition (5) of the spaces $\mathcal{X}$ and $\mathcal{Y}$ as follows:

$$\mathcal{X} = \mathbf{H}^1_0(\rho, \Omega) \times L^2(\rho, \Omega)/\mathbb{R}, \quad \mathcal{Y} = \mathbf{H}^1_0(\rho^{-1}, \Omega) \times L^2(\rho^{-1}, \Omega)/\mathbb{R}. \tag{64}$$

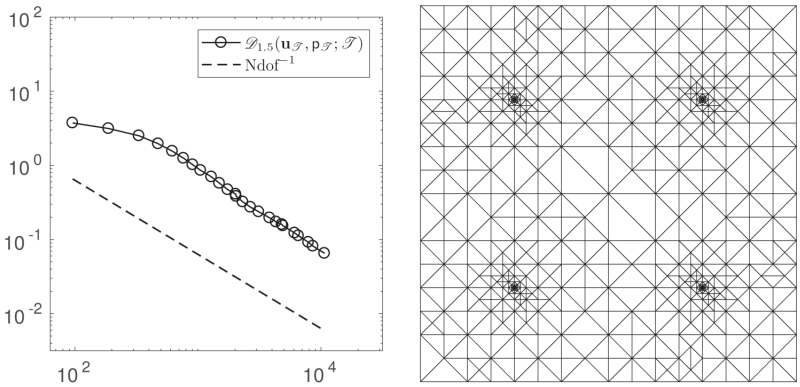

FIG. 5. A series of Dirac sources: *Experimental rate of convergence for the error estimator* $\mathscr{D}_{1.5}(\mathbf{u}_\mathscr{T}, \mathsf{p}_\mathscr{T}; \mathscr{T})$ *(left) and the mesh obtained after* 30 *adaptive refinements (right) with* $\alpha = 1.5$. *The mesh contains* 1324 *elements and* 693 *vertices.*

Define

$$D_{T,\mathcal{Z}} := \min_{z \in \mathcal{Z}} \left\{ \max_{x \in T} |x - z| \right\}. \tag{65}$$

We propose the following error estimator when the Taylor–Hood scheme is considered:

$$\mathscr{D}_\alpha(\mathbf{u}_\mathscr{T}, p_\mathscr{T}; \mathscr{T}) := \left(\sum_{T \in \mathscr{T}} \mathscr{D}_\alpha^2(\mathbf{u}_\mathscr{T}, p_\mathscr{T}; T) \right)^{\frac{1}{2}},$$

where the local indicators $\mathscr{D}_\alpha(\mathbf{u}_\mathscr{T}, p_\mathscr{T}; T)$ are such that

$$\begin{aligned} \mathscr{D}_\alpha(\mathbf{u}_\mathscr{T}, p_\mathscr{T}; T) := \Big(& h_T^2 D_{T,\mathcal{Z}}^\alpha \|\Delta \mathbf{u}_\mathscr{T} - (\mathbf{u}_\mathscr{T} \cdot \nabla)\mathbf{u}_\mathscr{T} - \operatorname{div} \mathbf{u}_\mathscr{T} \mathbf{u}_\mathscr{T} - \nabla \mathsf{p}_\mathscr{T}\|_{\mathbf{L}^2(T)}^2 \\ & + \|\operatorname{div} \mathbf{u}_\mathscr{T}\|_{L^2(\rho,T)}^2 + h_T D_{T,\mathcal{Z}}^\alpha \|[\![(\nabla \mathbf{u}_\mathscr{T} - \mathsf{p}_\mathscr{T} \mathbf{I})]\!] \cdot \boldsymbol{\nu}\|_{\mathbf{L}^2(\partial T \setminus \partial\Omega)}^2 + \sum_{z \in \mathcal{Z} \cap T} h_T^\alpha |\mathbf{F}_z|^2 \Big)^{\frac{1}{2}}. \end{aligned} \tag{66}$$

6.2.1. Convex domain with four Delta sources. We set $\Omega = (0,1)^2$ and

$$\mathcal{Z} = \{(0.25, 0.25), (0.25, 0.75), (0.75, 0.25), (0.75, 0.75)\}.$$

We consider, for all $z \in \mathcal{Z}$, $\mathbf{F}_z = (1,1)^\intercal$ and fix the exponent of the Muckenhoupt weight ρ as $\alpha = 1.5$.

In Figure 5 we present the experimental rates of convergence for the error estimator $\mathscr{D}_\alpha$ and the mesh obtained after 30 adaptive refinements with $\alpha = 1.5$. It can be observed that the devised a posteriori error estimator exhibits an optimal experimental rate of convergence. It can also be observed that most of the refinement is concentrated around the singular source points. In Figure 6, we present the finite element approximations of $|\mathbf{u}_\mathscr{T}|$ and $\mathsf{p}_\mathscr{T}$ over the mesh that is obtained after 30 iterations of our adaptive loop with $\alpha = 1.5$.

6.3. A convex domain with nonhomogeneous boundary conditions. We now explore the performance of our devised a posteriori error estimator by considering a problem with nonhomogeneous boundary conditions—a framework that does not fit in our analysis.

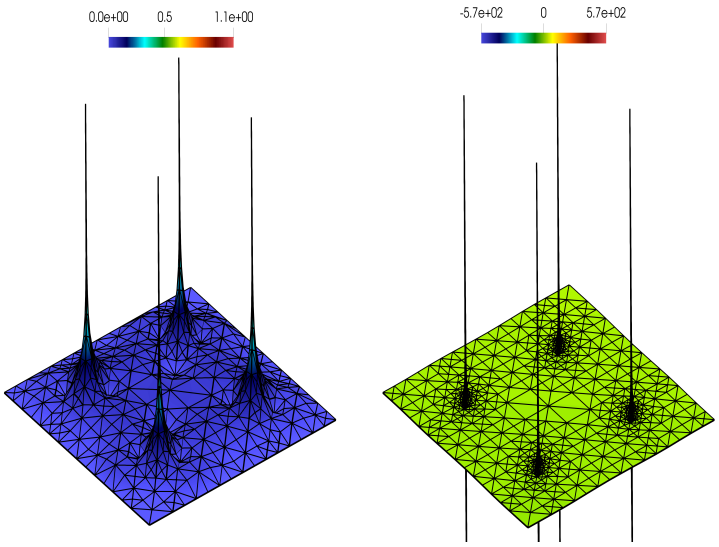

FIG. 6. A series of Dirac sources: *Finite element approximations* $|\mathbf{u}_{\mathscr{T}}|$ *(left) and* $\mathsf{p}_{\mathscr{T}}$ *(right) over the mesh obtained after* 30 *adaptive refinements with* $\alpha = 1.5$. *The mesh contains* 1324 *elements and* 693 *vertices.*

6.3.1. A rectangular domain. We set $\Omega = (0,4) \times (0,1)$, $z = (0.5, 0.5)^\intercal$, and $\mathbf{F} = (10,10)^\intercal$. The boundary conditions are illustrated in the left panel of Figure 7. We prescribe the parabolic Dirichlet inflow condition $\mathbf{u}_D = (y(1-y), 0)^\intercal$ on $\{0\} \times [0,1]$ and $\mathbf{u}_D = \mathbf{0}$ on $[0,4] \times \{0\} \cup \{1\}$ and the homogeneous Neumann condition $(\nabla \mathbf{u}_D - p\mathbf{I})\boldsymbol{\nu} = \mathbf{0}$ on $\{4\} \times (0,1)$. Here, $\boldsymbol{\nu}$ denotes the unit normal on $\partial\Omega$ pointing outwards. We recall that $\mathbf{I}$ denotes the identity matrix in $\mathbb{R}^{2\times 2}$.

In the right panel of Figure 7 we observe an optimal decay rate for the devised error estimator $\mathscr{E}_{1.5}(\mathbf{u}_{\mathscr{T}}, \mathsf{p}_{\mathscr{T}}; \mathscr{T})$. Finally, Figure 8 shows the streamlines associated to the velocity field $\mathbf{u}_{\mathscr{T}}$ and the mesh obtained after 30 adaptive refinements. It can be observed that most of the refinement is concentrated around the singular source point.

6.3.2. A rectangular domain with an obstacle. We set $\Omega = (0,10) \times (0,1) \setminus [2,4] \times [0.4, 0.6]$ and $\mathbf{F}_z = (10,10)^\intercal$ for $z \in \mathcal{Z}$, where $\mathcal{Z} = \{z_i\}_{i=1}^4$ with

$$z_1 = (1.011635, 0.198805)^\intercal, \quad z_2 = (1.011635, 0.801195)^\intercal,$$
$$z_3 = (5.354725, 0.200869)^\intercal, \quad z_4 = (5.264444, 0.719518)^\intercal.$$

The boundary conditions are illustrated in the top panel of Figure 9. We prescribe the parabolic Dirichlet inflow condition $\mathbf{u}_D = (y(1-y), 0)^\intercal$ on $\{0\} \times [0,1]$, $\mathbf{u}_D = \mathbf{0}$ on $[0,10] \times \{0\} \cup \{1\}$, and $\mathbf{u}_D = \mathbf{0}$ on the boundary of $[2,4] \times [0.4, 0.6]$, and the homogeneous Neumann condition $(\nabla \mathbf{u}_D - p\mathbf{I})\boldsymbol{\nu} = \mathbf{0}$ on $\{10\} \times (0,1)$. Here, $\boldsymbol{\nu}$ denotes the unit normal on $\partial\Omega$ pointing outwards. We recall again that $\mathbf{I}$ denotes the identity matrix in $\mathbb{R}^{2\times 2}$. The bottom panel of Figure 9 shows the experimental rate of convergence for the error estimator $\mathscr{D}_\alpha(\mathbf{u}_{\mathscr{T}}, \mathsf{p}_{\mathscr{T}}; \mathscr{T})$ with $\alpha = 1.5$. The estimator exhibits an optimal rate of decay. Finally, Figure 10 shows the streamlines associated to the velocity field $\mathbf{u}_{\mathscr{T}}$ over the mesh obtained after 100 iterations of our adaptive loop. It can be appreciated that most of the refinement is concentrated around the singular sources and the involved geometric singularities.

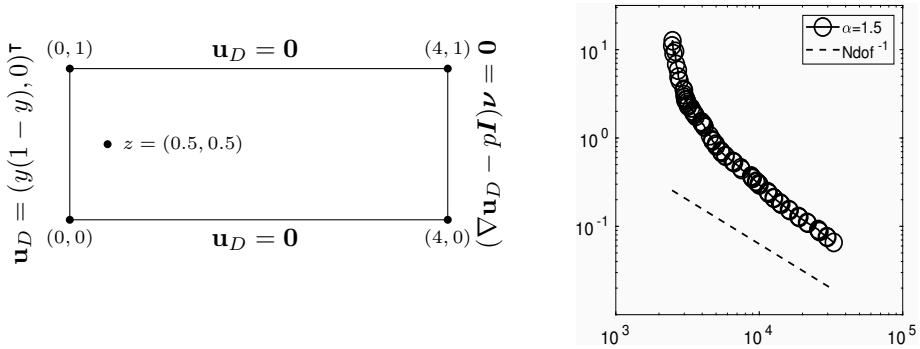

FIG. 7. A rectangular domain: *Boundary conditions for problem* (1) *on* $\Omega = (0,4) \times (0,1)$. *We prescribe the parabolic Dirichlet inflow condition* $\mathbf{u}_D = (y(1-y), 0)^\intercal$ *on* $\{0\} \times [0,1]$ *and* $\mathbf{u}_D = \mathbf{0}$ *on* $[0,4] \times \{0\} \cup \{1\}$ *and the homogeneous Neumann condition* $(\nabla \mathbf{u}_D - p\mathbf{I})\boldsymbol{\nu} = \mathbf{0}$ *on* $\{4\} \times (0,1)$ *(left). Experimental rate of convergence for the error estimator* $\mathscr{E}_\alpha(\mathbf{u}_\mathscr{T}, \mathsf{p}_\mathscr{T}; \mathscr{T})$ *with* $\alpha = 1.5$ *(right).*

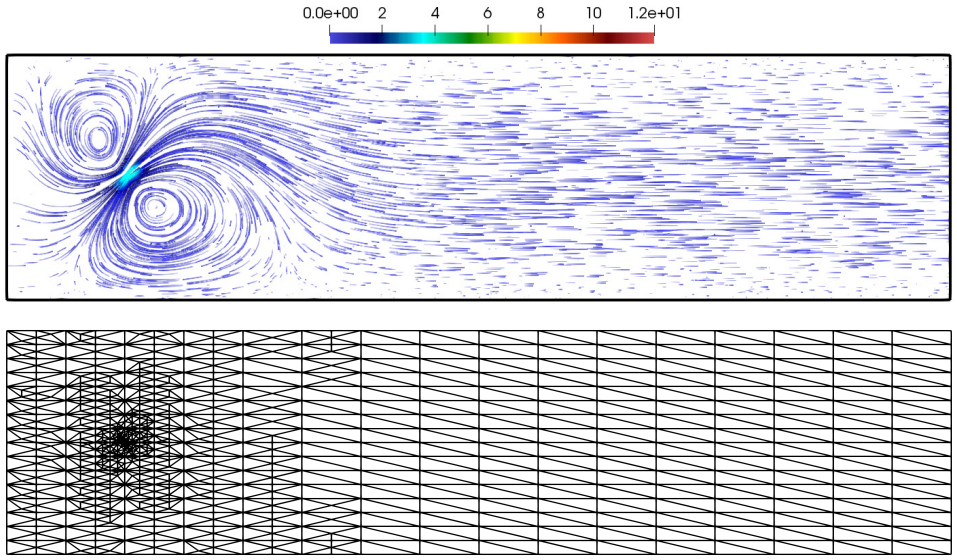

FIG. 8. A rectangular domain: *Streamlines associated to the velocity field* $\mathbf{u}_\mathscr{T}$ *(top) over the mesh, with* 1485 *elements and* 781 *vertices, that is obtained after* 30 *adaptive refinements of our adaptive loop (bottom). We have considered* $\alpha = 1.5$.

7. Concluding remarks. In this work, an a posteriori error estimator for the two dimensional stationary Navier–Stokes equations under singular forcing has been developed and analyzed. By singular forcing here we mean that the forcing is a linear combination of Dirac deltas in the interior of the domain. Under the standard smallness setting that guarantees uniqueness of solutions, we showed that this estimator is globally reliable and locally efficient. We presented several numerical examples to illustrate and extend our theory. To conclude we make the following observations.

- *Dependence on the constants on* α: In Proposition 3 and Theorems 9 and 11 we state that our estimates involve constants that depend on α and blow up as they

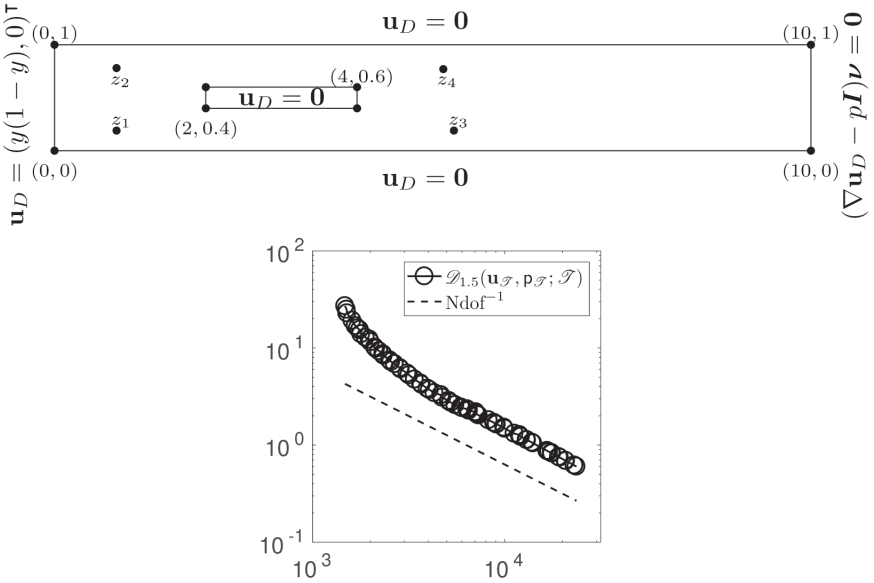

FIG. 9. A rectangular domain with an obstacle: *Boundary conditions for problem* (1) *on* $\Omega = (0,10) \times (0,1) \setminus [2,4] \times [0.4, 0.6]$. *We prescribe the parabolic Dirichlet inflow condition* $\mathbf{u}_D = (y(1-y),0)^\intercal$ *on* $\{0\} \times [0,1]$, $\mathbf{u}_D = \mathbf{0}$ *on* $[0,10] \times \{0\} \cup \{1\}$, $\mathbf{u}_D = \mathbf{0}$ *on the boundary of* $[2,4] \times [0.4, 0.6]$, *and the homogeneous Neumann condition* $(\nabla \mathbf{u}_D - p\mathbf{I})\boldsymbol{\nu} = \mathbf{0}$ *on* $\{10\} \times (0,1)$ *(top). Experimental rate of convergence for the error estimator* $\mathscr{D}_\alpha(\mathbf{u}_\mathscr{T}, \mathsf{p}_\mathscr{T}; \mathscr{T})$ *with* $\alpha = 1.5$ *(bottom).*

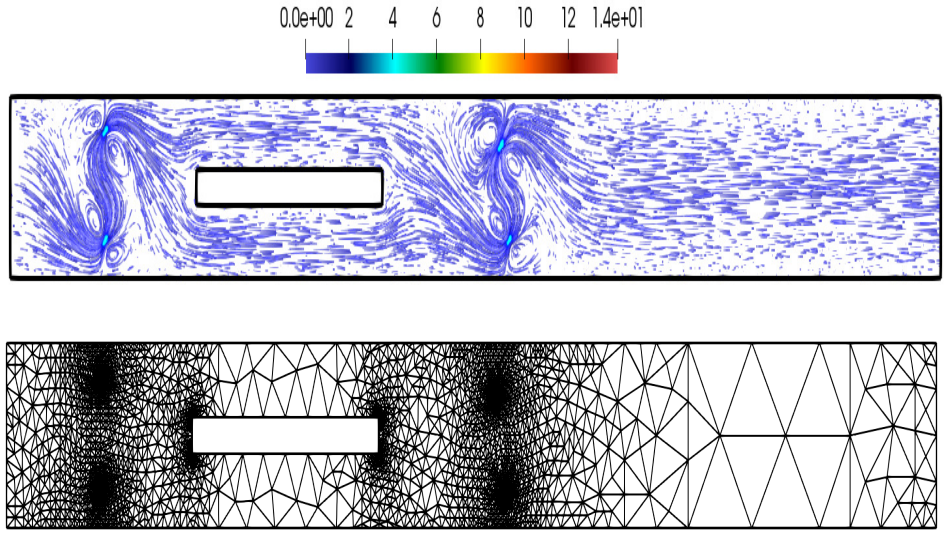

FIG. 10. A rectangular domain with an obstacle. *Streamlines associated to the velocity field* $\mathbf{u}_\mathscr{T}$ *(top) over the mesh, with* 8670 *elements and* 4498 *vertices, that is obtained after* 100 *adaptive refinements of our adaptive loop (bottom). We have considered* $\alpha = 1.5$.

approach the critical values 0 or 2. The precise value, or asymptotic behavior, of many of the constants that we use is not known, even for simple domains. In spite of this fact, the following comments can be provided.

- d_z^α belongs to the Muckenhoupt class A_2 provided $\alpha \in (-2, 2)$ and the Muckenhoupt characteristic of d_z^α blows up as $\alpha \to \pm 2$.
- The constants appearing in the interpolation estimates stated in Proposition 5, which are derived in [33], depend on the Muckenhoupt characteristic of d_z^α. It can thus be concluded that the involved constants blow up as $\alpha \to \pm 2$.
- In the course of the proof of Theorem 9 we use the precise bound for δ_z derived in [1, Theorem 4.7]. As is stated in [1, Theorem 4.7], the involved constant blows up as $\alpha \downarrow 0$. This is expected because δ_z does not belong to the dual of $H_0^1(\mathsf{d}_z^{-\alpha}, \Omega)$ when $\alpha = 0$; see [26, Remark 21.19] (see also the computation in [19, Proposition 5.2]).

These arguments lead us to the conclusion that in Proposition 3 and Theorems 9 and 11, the hidden constants blow up as α approaches either 0 or 2. However, as we previously stated, we have no control of all the involved constants (such as embedding constants between weighted Sobolev spaces), so it is not possible to make quantitative statements regarding the behavior of these constants and, as a consequence, of the behavior of our estimator as α approaches either 0 or 2.

- *Practical choice of* α: The numerical observations seem to indicate (see Figures 2 and 4) that the choice of $\alpha \in (0, 2)$ is not essential for the asymptotic behavior of the method, but a better value of the error at a fixed mesh can be obtained for values of α closer to two. One may not wish to make this value too close to the critical value of two, however, as this may give a blowup in the implicit constants that appear in our estimates. When the domain exhibits geometric singularities, numerical evidence supports the claim that they are rapidly noticed for values of α closer to two. In such a case the refinement is more spread throughout the domain due to the smaller relative importance of the singularity introduced by δ_z.
- *Limitations:* There seem to be two main limitations to our approach. First, we are restricted to the two dimensional setting. The reason for this is explained in Remark 2. Our current arguments based on weighted spaces and related techniques cannot show the boundedness of the convective term in three dimensions. Note that a similar limitation appears in [12, 32]. The second limitation is that we need to know the location and intensity of the Dirac source for our approach to work. However, if we do not have these two pieces of information we do not know the forcing term, a problem that is beyond our scope here. We are not claiming that our estimator works for any singular forcing term, or that it will perform well if the forcing happens to be regular. In fact, in this case our estimator *will not work*. This is a heavily tailored estimator for a very singular problem.
- *Boundedness of* $\{\mathcal{S}_{\mathscr{T}}^{-1}\}_{\mathscr{T}\in\mathbb{T}}$: Our developments are based on the fact that the family $\{\mathcal{S}_{\mathscr{T}}^{-1}\}_{\mathscr{T}\in\mathbb{T}}$ is uniformly bounded on weighted spaces. As mentioned above, if Ω is convex and $\mathbb{T}$ is quasi-uniform, then [19, Theorem 4.1] has proved this fact. While convexity may not be a restrictive assumption on the domain, the fact that $\mathbb{T}$ must be quasi-uniform is not fulfilled in an adaptive setting. Filling this gap is beyond the scope of our interest here. Our numerical experiments, however, present numerical evidence that this assumption is indeed true. If this assumption is false, the constants in our estimates will depend on $\mathscr{T}$ (read number of degrees of freedom), and the devised adaptive loop will not deliver optimal asymptotic rates of decay.

REFERENCES

[1] J. P. Agnelli, E. M. Garau, and P. Morin, *A posteriori error estimates for elliptic problems with Dirac measure terms in weighted spaces*, ESAIM Math. Model. Numer. Anal., 48 (2014), pp. 1557–1581, https://doi.org/10.1051/m2an/2014010.

[2] H. Aimar, M. Carena, R. Durán, and M. Toschi, *Powers of distances to lower dimensional sets as Muckenhoupt weights*, Acta Math. Hungar., 143 (2014), pp. 119–137, https://doi.org/10.1007/s10474-014-0389-1.

[3] M. Ainsworth and J. T. Oden, *A posteriori error estimators for the Stokes and Oseen equations*, SIAM J. Numer. Anal., 34 (1997), pp. 228–245, https://doi.org/10.1137/S0036142994264092.

[4] A. Allendes, E. Otárola, R. Rankin, and A. J. Salgado, *Adaptive finite element methods for an optimal control problem involving Dirac measures*, Numer. Math., 137 (2017), pp. 159–197, https://doi.org/10.1007/s00211-017-0867-9.

[5] A. Allendes, E. Otárola, and A. J. Salgado, *A posteriori error estimates for the Stokes problem with singular sources*, Comput. Methods Appl. Mech. Engrg., 345 (2019), pp. 1007–1032, https://doi.org/10.1016/j.cma.2018.11.004.

[6] P. R. Amestoy, I. S. Duff, J.-Y. L'Excellent, and J. Koster, *A fully asynchronous multifrontal solver using distributed dynamic scheduling*, SIAM J. Matrix Anal. Appl., 23 (2001), pp. 15–41, https://doi.org/10.1137/S0895479899358194.

[7] P. R. Amestoy, A. Guermouche, J.-Y. L'Excellent, and S. Pralet, *Hybrid scheduling for the parallel solution of linear systems*, Parallel Comput., 32 (2006), pp. 136–156, https://doi.org/10.1016/j.parco.2005.07.004.

[8] D. N. Arnold, F. Brezzi, and M. Fortin, *A stable finite element for the Stokes equations*, Calcolo, 21 (1984), pp. 337–344, https://doi.org/10.1007/BF02576171.

[9] S. Bertoluzza, A. Decoene, L. Lacouture, and S. Martin, *Local error analysis for the Stokes equations with a punctual source term*, Numer. Math., 140 (2018), pp. 677–701, https://doi.org/10.1007/s00211-018-0976-0.

[10] F. Boyer and P. Fabrie, *Mathematical Tools for the Study of the Incompressible Navier-Stokes Equations and Related Models*, Appl. Math. Sci. 183, Springer, New York, 2013, https://doi.org/10.1007/978-1-4614-5975-0.

[11] M. Bulíček, J. Burczak, and S. Schwarzacher, *A unified theory for some non-Newtonian fluids under singular forcing*, SIAM J. Math. Anal., 48 (2016), pp. 4241–4267, https://doi.org/10.1137/16M1073881.

[12] E. Casas and K. Kunisch, *Optimal control of the two-dimensional stationary Navier–Stokes equations with measure valued controls*, SIAM J. Control Optim., 57 (2019), pp. 1328–1354, https://doi.org/10.1137/18M1185582.

[13] S.-K. Chua, *Weighted Sobolev inequalities on domains satisfying the chain condition*, Proc. Amer. Math. Soc., 117 (1993), pp. 449–457, https://doi.org/10.2307/2159182.

[14] P. G. Ciarlet, *The Finite Element Method for Elliptic Problems*, SIAM, Philadelphia, 2002, https://doi.org/10.1137/1.9780898719208.

[15] P. Clément, *Approximation by finite element functions using local regularization*, Rev. Française Automat. Informat. Recherche Opérationnelle Sér., 9 (1975), pp. 77–84.

[16] I. Drelichman, R. G. Durán, and I. Ojea, *A weighted setting for the numerical approximation of the Poisson problem with singular sources*, SIAM J. Numer. Anal., 58 (2020), pp. 590–606, https://doi.org/10.1137/18M1213105.

[17] J. Duoandikoetxea, *Fourier Analysis*, Grad. Stud. Math. 29, American Mathematical Society, Providence, RI, 2001 (translated and revised from the 1995 Spanish original by David Cruz-Uribe).

[18] R. Durán and F. López García, *Solutions of the divergence and Korn inequalities on domains with an external cusp*, Ann. Acad. Sci. Fenn. Math., 35 (2010), pp. 421–438, https://doi.org/10.5186/aasfm.2010.3527.

[19] R. G. Durán, E. Otárola, and A. J. Salgado, *Stability of the Stokes projection on weighted spaces and applications*, Math. Comp., 89 (2020), pp. 1581–1603, https://doi.org/10.1090/mcom/3509.

[20] R. G. Durán and A. L. Lombardi, *Error estimates on anisotropic Q_1 elements for functions in weighted Sobolev spaces*, Math. Comp., 74 (2005), pp. 1679–1706, https://doi.org/10.1090/S0025-5718-05-01732-1.

[21] A. Ern and J.-L. Guermond, *Theory and Practice of Finite Elements*, Appl. Math. Sci. 159, Springer-Verlag, New York, 2004.

[22] E. B. Fabes, C. E. Kenig, and R. P. Serapioni, *The local regularity of solutions of degenerate elliptic equations*, Comm. Partial Differential Equations, 7 (1982), pp. 77–116, https://doi.org/10.1080/03605308208820218.

[23] R. Farwig and H. Sohr, *Weighted L^q-theory for the Stokes resolvent in exterior domains*, J. Math. Soc. Japan, 49 (1997), pp. 251–288.
[24] V. Girault and P.-A. Raviart, *Finite Element Methods for Navier-Stokes Equations. Theory and Algorithms*, Springer Ser. Comput. Math. 5, Springer-Verlag, Berlin, 1986, https://doi.org/10.1007/978-3-642-61623-5.
[25] V. Gol'dshtein and A. Ukhlov, *Weighted Sobolev spaces and embedding theorems*, Trans. Amer. Math. Soc., 361 (2009), pp. 3829–3850, https://doi.org/10.1090/S0002-9947-09-04615-7.
[26] J. Heinonen, T. Kilpeläinen, and O. Martio, *Nonlinear Potential Theory of Degenerate Elliptic Equations*, Dover, Mineola, NY, 2006 (unabridged republication of the 1993 original).
[27] P. Hood and C. Taylor, *Navier-Stokes equations using mixed interpolation*, in Finite Element Methods in Flow Problems, University of Alabama Press, Huntsville, 1974, pp. 121–132.
[28] R. Hurri-Syrjänen, *A weighted Poincaré inequality with a doubling weight*, Proc. Amer. Math. Soc., 126 (1998), pp. 545–552, https://doi.org/10.1090/S0002-9939-98-04059-3.
[29] I. Kossaczký, *A recursive approach to local mesh refinement in two and three dimensions*, J. Comput. Appl. Math., 55 (1994), pp. 275–288, https://doi.org/10.1016/0377-0427(94)90034-5.
[30] V. Kozlov, V. Maz'ya, and J. Rossmann, *Elliptic Boundary Value Problems in Domains with Point Singularities*, American Mathematical Society, Providence, RI, 1997.
[31] L. Lacouture, *A numerical method to solve the Stokes problem with a punctual force in source term*, Comptes Rendus Mécanique, 343 (2015), pp. 187–191, https://doi.org/10.1016/j.crme.2014.09.008.
[32] F. Lepe, E. Otárola, and D. Quero, *Error estimates for FEM discretizations of the Navier–Stokes equations with Dirac measures*, submitted.
[33] R. H. Nochetto, E. Otárola, and A. J. Salgado, *Piecewise polynomial interpolation in Muckenhoupt weighted Sobolev spaces and applications*, Numer. Math., 132 (2016), pp. 85–130, https://doi.org/10.1007/s00211-015-0709-6.
[34] E. Otárola and A. J. Salgado, *The Poisson and Stokes problems on weighted spaces in Lipschitz domains and under singular forcing*, J. Math. Anal. Appl., 471 (2019), pp. 599–612, https://doi.org/10.1016/j.jmaa.2018.10.094.
[35] E. Otárola and A. J. Salgado, *A weighted setting for the stationary Navier Stokes equations under singular forcing*, Appl. Math. Lett., 99 (2020), 105933, https://doi.org/10.1016/j.aml.2019.06.004.
[36] K. Schumacher, *Solutions to the equation* $\operatorname{div} u = f$ *in weighted Sobolev spaces*, in Parabolic and Navier-Stokes Equations, Part 2, Banach Center Publ. 81, Polish Acad. Sci. Inst. Math., Warsaw, 2008, pp. 433–440, https://doi.org/10.4064/bc81-0-26.
[37] K. Schumacher, *The instationary Navier-Stokes equations in weighted Bessel-potential spaces*, J. Math. Fluid Mech., 11 (2009), pp. 552–571, https://doi.org/10.1007/s00021-008-0272-3.
[38] L. R. Scott and S. Zhang, *Finite element interpolation of nonsmooth functions satisfying boundary conditions*, Math. Comp., 54 (1990), pp. 483–493, https://doi.org/10.2307/2008497.
[39] H. Sohr, *The Navier-Stokes Equations. An Elementary Functional Analytic Approach*, Birkhäuser Adv. Texts Basler Lehrbücher, Birkhäuser Verlag, Basel, 2001, https://doi.org/10.1007/978-3-0348-8255-2.
[40] L. Tartar, *An Introduction to Navier-Stokes Equation and Oceanography*, Lect. Notes Unione Mat. Italiana 1, Springer-Verlag, Berlin; UMI, Bologna, 2006, https://doi.org/10.1007/3-540-36545-1.
[41] R. Temam, *Navier-Stokes Equations. Theory and Numerical Analysis*, AMS Chelsea Publishing, Providence, RI, 2001, https://doi.org/10.1090/chel/343 (reprint of the 1984 edition).
[42] B. O. Turesson, *Nonlinear Potential Theory and Weighted Sobolev Spaces*, Lecture Notes in Math. 1736, Springer-Verlag, Berlin, 2000, https://doi.org/10.1007/BFb0103908.
[43] A. I. Tyulenev, *The problem of traces for Sobolev spaces with Muckenhoupt-type weights*, Math. Notes, 94 (2013), pp. 668–680 (in English), https://doi.org/10.1134/S0001434613110084; Mat. Zametki, 94 (2013), pp. 720–732 (in Russian).
[44] A. I. Tyulenev, *Description of traces of functions in the Sobolev space with a Muckenhoupt weight*, Proc. Steklov Inst. Math., 284 (2014), pp. 280–295 (in English), https://doi.org/10.1134/S0081543814010209; Tr. Mat. Inst. Steklova, 284 (2014), pp. 288–303 (in Russian).
[45] R. Verfürth, *A posteriori error estimators for the Stokes equations*, Numer. Math., 55 (1989), pp. 309–325, https://doi.org/10.1007/BF01390056.
[46] R. Verfürth, *A Posteriori Error Estimation Techniques for Finite Element Methods*, Numer. Math. Sci. Comput., Oxford University Press, Oxford, 2013, https://doi.org/10.1093/acprof:oso/9780199679423.001.0001.